ADDIS ABABA UNIVERSITY

SCHOOL OF GRADUATE STUDIES

INSTITUTE OF TECHNOLOGY

ELECTRICAL AND COMPUTER ENGINEERING DEPARTMENT

Performance evaluation of a layered space-time structure for MIMO systems

By

Getaneh Birlew

Advisor

Dr.-Ing Hailu Ayele

A Thesis Submitted to the School of Graduate Studies of Addis Ababa University in Partial Fulfillment of the Requirements for the Degree of Masters of Science in Electrical Engineering

July, 2011
Addis Ababa, Ethiopia

ADDIS ABABA UNIVERSITY SCHOOL OF GRADUATE STUDIES

INSTITUTE OF TECHNOLOGY

ELECTRICAL AND COMPUTER ENGINEERING DEPARTMENT

Performance evaluation of a layered space-time structure for MIMO systems

By

Getaneh Birlew

Approval by Board of Examiners

_____	_____
Chairman, Dept. Graduate Committee	Signature
Dr.-Ing Hailu Ayele	_____
Advisor	Signature
Ato Yialemzewd Negash (PHD candidate)	_____
Internal Examiner	Signature
Dr.-Ing Dereje Hailemariam	_____
External Examiner	Signature

Declaration

I, the undersigned, declare that this thesis is my original work, has not been presented for a degree in this or any other university, and all sources of materials used for the thesis have been fully acknowledged.

Getaneh Birlew _____

Name Signature

Place: Addis Ababa

Date of Submission: _____

This thesis has been submitted for examination with my approval as a university advisor.

Dr.-Ing Hailu Ayele _____

Advisor's Name Signature

Acknowledgement

I want to thank my advisor Dr.Ing Hailu Ayele for his insightful advice and comments from deciding the thesis topic to revising the report, as well as his consistent encouragement throughout the whole time of this thesis project. Above all, he is a model instructor in the teaching profession. Finally I would like to thank my parents for their support throughout my project.

Table of contents

Table of Figures

List of Tables

List of Acronyms

3GPP 3G Partnership Project

4G Fourth Generation

AWGN Additive White Gaussian Noise

BER Bit Error Rate

BLAST Bell Lab Layered Space Time

BPSK Binary Phase Shift Key

CSI Channel State Information

dB Deci Bell

D-BLAST Diagonal BLAST

IEEE Institute of Electrical and Electronics Engineers

i.i.d independent, identically distributed

LOS line of sight

LST Layered Space Time

MIMO Multiple Input Multiple Output

MISO Multiple Input Single Output

ML Maximum Likelihood

MMSE Minimum Mean Square Error

MMSE-SIC Minimum Mean Square Error with Successive Interference Cancellation

NLOS Non-Line-Of Sight

OSIC Ordered Successive Interference Cancellation

QAM Quadrature Amplitude Modulation

RCPC Rate Compatible Punctured Convolutional codes

RX Receiver

SD Spatial Diversity

SIC Successive Interference Cancellation

SIMO Single Input Multiple Output

SISO Single Input Single Output

SM Spatial Multiplexing

SNR Signal to Noise Ratio

STBC Space Time Block Code

SVD Singular Value Decomposition

TX Transmitter

V-BLAST Vertical BLAST

VB Viterbi algorithm

ZF Zero Forcing

ZF-SIC Zero Forcing with Successive Interference Cancellation

Abstract

MIMO systems are an appealing candidate for emerging fourth-generation wireless networks due to their potential to exploit space diversity for increasing conveyed throughput without wasting bandwidth and power resources. Particularly, layered space-time architecture (LST) proposed by Foschini, is a technique to achieve a significant fraction of the theoretical capacity with a reasonable implementation complexity. It is based on signal processing and conventional one dimensional coding, which includes vertical BLAST (*Bell Laboratories Layered Space Time*) and diagonal BLAST. BLAST accomplishes this by splitting a single user's data stream into multiple sub-streams and using an array of transmitter antennas to simultaneously launch the parallel sub-streams. All sub-streams are transmitted in the same frequency band, so spectrum is used very efficiently. Since the user's data is being sent in parallel over multiple antennas, the effective transmission rate is increased roughly in proportion to the number of antenna elements used.

In this thesis, we focus on the performance evaluation of a layered space-time structure for MIMO systems under Rayleigh fading condition. Firstly, we throughly understand the different layered space-time architectures and investigate the performance of general V-BLAST architecture with Maximum Likelihood (ML), Zero-Forcing (ZF), Minimum Mean-Square Error (MMSE), the Successive Interference Cancellation (SIC) and the Ordered Successive Interference Cancellation (OSIC) detectors for $2 \times n_R$ antenna arrangement. Here, in addition to performance (BER), the different detection algorithms are evaluated in terms of computational complexity. From the results, we have seen that the maximum-likelihood (ML) detector is optimum in the sense of achieving the minimum error probability. Unfortunately, the complexity of the ML detector is exponential in the constellation size and the dimensions of the system. But, by using the SIC & OSIC detectors, we approach the performance of the ML detector with lower computational complexity. It is also shown that the average performance is improved when the number of receive antenna increases. Finallly we understand and evaluate performance bound trends of Rate Compatible Punctured Convolutional (RCPC) codes and investigate the unequal error protection capabilities of rate compatible punctured convolutional codes (RCPC codes) when used together with V-BLAST MIMO systems for a mother code rate of 1/4. The results show that as the rate of a code decreases, the error-protection level improves consistently.

Key words: ML, MMSE , ZF, V-BLAST, MIMO, SIC, OSIC and RCPC codes

Chapter 1

Introduction

In this new information age, high data rate and strong reliability features of wireless communication systems are becoming the dominant factors for a successful deployment of commercial networks. The multiple-input multiple-output (MIMO) scheme in wireless communication is one prominent candidate that fulfills this need, mainly due to its high capacity which does not call for bandwidth expansion [1, 2, 12]. The accomplishment of this high-capacity potential needs an appropriate signal processing architecture. Bell Labs Layered Space Time Architecture (BLAST) is an extraordinary bandwidth efficient approach to wireless communication which takes advantage of the spatial dimension by transmitting and detecting a number of independent co-channel data streams using multiple but essentially co-located antennas. This new communication structure targets application in future generations of wireless systems, bringing high bit rates to the office and home.

An architecture which theoretically achieves the highest capacity was proposed as BLAST in [2] and it attains the spectral efficiencies up to 42 bits/sec/Hz. This represents a spectacular increase compared to currently achievable spectral efficiencies of 2-3 bits/sec/Hz, in cellular mobile and wireless LAN systems [8]. The original diagonal-BLAST version used a cyclic association of data streams, called layers, with transmit antennas, thereby producing an "averaged" channel which is the same for all layers. Difficulties in the realization of D-BLAST led to a modified architecture called V-BLAST [10], where each layer is associated with certain transmit antenna (as shown in Figure 1.1).

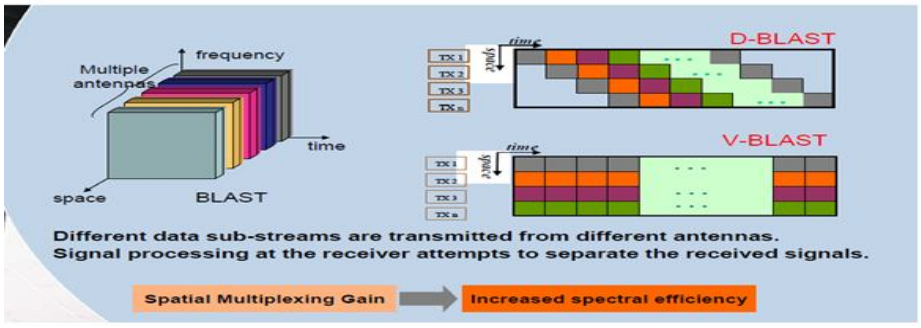

Figure 1.1: Layer and transmit antenna association of V-BLAST and D-BLAST structure [14]

1.1 Motivation

It is commonly known that at the receiver side the best performance can be achieved when a full maximum likelihood search is performed over the complete dimensions that are spanned by the space-time encoding process. It is obvious that the complexity of such a receiver grows exponentially with the size of the spatial and temporal dimension [1, 2, 8]. Especially, when the space-time codeword sizes result in unmanageable complexity, a search for less complex receiver architecture is required. But in general less complex receiver schemes result in a performance loss. The fundamental problem of MIMO systems is the mapping operation at the transmitter and the corresponding inversion at the receiver to optimize the overall performance of the wireless system. Issues relating to the following system parameters are performance metrics for wireless communication [1, 5]: bit rate, reliability and complexity.The goal is to have a receiver with a manageable complexity that performs closely to the maximum likelihood bound and provides the highest possible bit rate per unit bandwidth.

In addition, the design of an error protection scheme usually consists of selecting a fixed channel code with a certain rate, complexity, and correction capability that is uniform for all the data to be transmitted. Further, the fixed code is constructed for the average or worst case channel conditions to be expected [16, 21, 23]. However, in many cases, the data to be transmitted has different error protection needs. One way to achieve unequal error protection (UEP) is to arrange the binary information bits in groups according to their error sensitivity and a number of channel encoders and decoders are employed, in parallel, to provide the necessary error protection levels [13]. The complexity of this scheme becomes impractical when the number of error protection levels becomes large. Thus, a single channel encoder and decoder structure using rate compatible punctured convolutional (RCPC) codes are recommended for this application.

1.2 Objective

The objective of this work is to investigate the performance of a layered space-time structure for MIMO systems. The performance analysis in terms of bit error rate (BER) vs signal to noise ratio (SNR) under Rayleigh fading condition will be presented with simulation results. It includes the following:

- Thoroughly understanding the different layered space-time architectures and their distinguishing features.
- To understand and evaluate performance of V-BLAST system. Here we study & investigate the performance of general V-BLAST architecture with Maximum Likelihood (ML), Zero-Forcing (ZF), Minimum Mean-Square Error (MMSE), the Successive Interference Cancellation (SIC) and the Ordered Successive Interference Cancellation (OSIC) detectors. The final goal is to provide the researcher or system designer an insight to make comparison and tradeoff (performance versus complexity) studies among the various detectors so as to determine the optimum choice in the face of his or her available constraints.
- To understand and evaluate performance bound trends of Rate Compatible Punctured Convolutional (RCPC) codes by using the code performance parameters.
- To understand and evaluate performance of RCPC encoded V-BLAST system. In many source coding schemes, the effect of a channel error varies significantly from one bit to another. Hence, to make the best available use of the limited channel coding redundancy, unequal error protection is needed. In this thesis, we study the unequal error protection capabilities of RCPC codes when used together with V-BLAST MIMO systems.

1.3 Litrature review

In recent years, the use of multiple-input multiple-output (MIMO) wireless technologies that offer significant promise in achieving high data rates over wireless links has captured a lot of interest. G.J. Foschini showed that the capacity can be improved by a factor equal to the minimum number of transmit and receive antennas if perfect channel state information (CSI) is available at the receiver, compared with a single-input single-output (SISO) system with flat Rayleigh fading channels [2].

BLAST systems demand powerful signal processing procedures to recover the signal transmitted by the antenna arrays, such that the potential advantages of the BLAST system can be guaranteed and the BLAST system will work in the best possible way. Numerous detection algorithms are proposed for this architecture. G.J. Foschini *et al.* [7, 9] implemented linear combinatorial nulling, in which each substream in turn is considered to be the desired signal one

after another, and the remaining substreams are considered as ”interferers”. Nulling is performed by linearly weighting the received signals so as to satisfy ZF criterion. Stephen Baro *et al* [28] provided another way to improve detection performance values by replacing the ZF nulling by the MMSE algorithm.

Different coding methods are used to achieve the great potential of BLAST MIMO systems. Stephen Baro et al [28] applied transmit diversity with space-time block codes and showed that the number of receive antennas can be reduced and the diversity level increased compared to the original BLAST. In many wireless communication systems, convolutional codes are widely used due to their capability that enable soft-decision decoding and their near Shannon-capacity performance [20]. However the complexity in their decoding process tends to increase with each additional bit in the encoder output, and this may lead to erroneous decoding. Use of punctured convolutional codes is one way of solving this problem and latter on they developed into RCPC codes, in which code rates can be adapted to the protection levels of the transmitted data using single encoder and decoder structure [3]. R. Guo et al [6] report that an RCPC encoded MIMO system outperforms the MIMO system without RCPC encoding. Yujin Noh et al [13] has proposed unequal error protection (UEP) for MIMO-OFDM system. The UEP is attained by using multiple encoders which results in a complex system and this leaves a room for system simplification in terms of RCPC usage. The above researches do not cover a layered architecture to boost the capacity of the MIMO system. Lydia Sari et al [4] report that RCPC-encoded V-BLAST MIMO system under the general Nakagami-m Fading channel model has robust performance and numerical simulation results show that the use of RCPC codes increases the robustness of the system, even under severe fading condition. The V-BLAST scheme in [4] is based on automatic repeat request (ARQ) and channel state information (CSI) is fed onto the transmitter block by singular value decompsition (SVD), which in turn allocates the code rate to the transmit antennas, according to the condition of the sub-channel. For wireless communication systems where channel state information feedback is typically not implemented, there is a need for a different way to have unequal error protection.

In this thesis, we study different detection algorithms for layered space-time MIMO systems over Rayleigh fading channels, and implement them in Matlab software. Here, we focus on the V-BLAST structure. Our main interest is the bit error rate and complexity of different detection methods. ZF, MMSE and ML are used as detection algorithms. SIC is used instead of joint detection in order to reduce the complexity. An ordered SIC detector is also used to combat the influence of error propagation. Finally, we investigate performance bound trends of RCPC codes and the unequal error protection capabilities of RCPC codes when used together with V-BLAST MIMO systems by using single encoder/decoder pair for a mother code rate of 1/4.

1.4 Thesis organization

The rest of the thesis is organized as follows. We begin in Chapter 2 with a brief overview of MIMO systems. The primary goal of this chapter is to introduce basic concepts, models and notations that will be used throughout the thesis.

In Chapter 3, firstly we throughly introduce the different layered space-time architectures and investigate the performance of general V-BLAST architecture with ML, ZF, MMSE, SIC and OSIC detectors. Another method that is used to compare the different detectors is by determining the complexity in terms of number of additions and multiplications.The resulting complexity numbers are a good measure for the final complexity of the receiver. Finallly, we understand and evaluate performance bound trends of RCPC codes and study the unequal error protection capabilities of RCPC codes when used together with V-BLAST MIMO systems for a mother code rate of 1/4.

In Chapter 4, simulation results for the performance of general V-BLAST architecture, performance bound trends of RCPC codes by using the code performance parameters and performance of RCPC encoded V-BLAST system under Rayleigh fading condition is presented. Detail analysis of the simulation outputs is also given here. The conclusion of the thesis is summarized in Chapter 5, where some suggestions are also indicated for further research of this area.

Chapter 2

Basics of MIMO systems

2.1 Introduction

During the past decades, wireless communication has benefitted from substantial advances and it is considered as the key enabling technique of innovative future consumer products. For the sake of satisfying the requirements of various applications, significant technological achievements are required to ensure that wireless devices have appropriate architectures suitable for supporting a wide range of services delivered to the users. It has been deployed through out the world to help people and machines to communicate with each other independent of their location [5, 33]. *"Always best connected"* is one of the slogans for the fourth generation of wireless communications system (4G), meaning that your wireless equipment should connect to the network or system that is the "best" for you at the moment.

There are two fundamental aspects of wireless communication that make the problem challenging and interesting [1, 5, 26]. These aspects are by and large not as significant in wire line communication. First, the phenomenon of *fading*: the time-variation of the channel strengths due to the small-scale effect of multipath fading, as well as larger scale effects such as path loss via distance attenuation and shadowing by obstacles. Second, unlike in the wired world where each transmitter-receiver pair can often be thought of as an isolated point-to-point link, wireless users communicate over the air and there is significant *interference* between them in wireless communication. The interference can be between transmitters communicating with a common receiver (e.g. uplink of a cellular system), between signals from a single transmitter to multiple receivers (e.g. downlink of a cellular system), or between different transmitter-receiver pairs (e.g. interference between users in different cells). Therefore, wireless systems must be designed to mitigate the effect of fading and interference to guarantee a reliable communication.

In wireless communications, spectrum is a scarce resource that imposes a high cost on the high data rate transmission [5, 8]. Fortunately, the emergence of multiple antenna system has opened another very resourceful dimension – space, for information transmission in the air. It has been demonstrated that a multiple antenna system provides very promising gain in capacity without

increasing the spectrum, reliability, throughput, power consumption and less sensitivity to fading, hence leading to a breakthrough in the data rate of wireless communication systems [2]. As a consequence, MIMO systems have become one of the major focuses in the research community of wireless communications and information theory.

Different MIMO architectures provide different benefits which can be broadly classified as array gain, interference reduction, diversity gain and multiplexing gain.

- **Array gain**: is the average increase in *signal-to-noise ratio* (SNR) at the receiver that can be obtained by the coherent combining of multiple antenna signals at the receiver or at the transmitter side or at both sides. The average increase in signal power is proportional to the number of receive antennas [26]. In case of multiple antennas at the transmitter, array gain exploitation requires channel knowledge at the transmitter.
- **Interference reduction**: In contrast to copper or optical fiber, the wireless medium is an unguided communication link as a result of which co-channel interference is a frequent problem. Co-channel interference contributes to the overall noise of the system and degrades performance. By using multiple antennas it is possible to suppress interfering signals leading to an improvement of *system capacity*. Interference reduction requires knowledge of the channel of the desired signal; but exact knowledge of channel may not be necessary [26].
- **Diversity gain**: An effective method to combat fading is diversity. According to the domain where diversity is introduced, diversity techniques are classified into time, frequency and space diversity [33]. Space or antenna diversity has been popular in wireless microwave communications and can be classified into two categories: receive diversity and transmit diversity [1], depending on whether multiple antennas are used for reception or transmission.
    - ✓ Receive Diversity: It can be used in channels with multiple antennas at the receive side. The receive signals are assumed to fade independently and are combined at the receiver so that the resulting signal shows significantly reduced fading. Receive diversity is characterized by the number of

independent fading branches and it is at most equal to the number of receive antennas.

- ✓ Transmit Diversity: Transmit diversity is applicable to channels with multiple transmit antennas and it is at most equal to the number of the transmit antennas, especially if the transmit antennas are placed sufficiently apart from each other. Data is processed at the transmitter and then spread across the multiple antennas.

In the case of multiple antennas at both ends, utilization of diversity requires a combination of the receive and transmit diversity as explained above. The diversity order is bounded by the product of the number of transmit and receive antennas, if the channel between each transmit-receive antenna pair fades independently [34].

The key feature of all diversity methods is a low probability of simultaneous deep fades in the various diversity channels. In general the system performance with diversity techniques depends on how many signal replicas are combined at the receiver to increase the overall SNR. There exist four main types of signal combining methods at the receiver: selection combining, switched combining, equal-gain combining and maximum ratio combining (MRC). More information about combining methods can be found in [5, 26].

- **Multiplexing gain**: The key differentiating advantage of MIMO systems is practical throughput enhancement which is not provided by single-input multiple-output (SIMO) or multiple-input single- output (MISO) systems. We refer to this leverage as multiplexing gain and it can be realized through a technique known as spatial multiplexing [2].

Wireless systems consisting of a transmitter, a radio channel and a receiver are categorized by their number of inputs and outputs [33]. Communication systems with one transmit and one receive antenna are called single-input single-output (SISO) system. When several antennas are available at the transmitter side while the receiver has only one antenna, we refer to the system as MISO systems. In the same way, systems with one transmit and several receive antennas are called SIMO systems. We are most interested in systems with more than one antenna at both

transmitter and receiver sides, namely, MIMO systems. The MIMO system is the most general and includes SISO,MISO, SIMO systems as special cases.

2.2 Modeling the Wireless MIMO System

To analyze the wireless communication system, appropriate models for signals and channels are needed. In this section, we will present the necessary background for the models used in the thesis. We will give an overview of the MIMO channels, the signal models and describe SNR definition.

2.2.1 Channel and System Model

Generally, a MIMO system consists of n_T transmit and n_R receive antennas (Figure 2.1). It is called a MIMO (n_T, n_R) system. The transmitted signals for a MIMO system with n_T transmit antennas can be generated by performing the following tasks on the incoming bit stream [8, 33]:

- channel encoding.
- Mapping of the encoded bits on the spatial and/or temporal dimension.
- Modulation.

All the transmit antennas send their signals simultaneously in the same bandwidth of the radio channel. Each receive antenna receives the superposition of all the transmit signals disturbed by the noise in the radio channel. If no more than min [n_T, n_R] independent signals are transmitted, they can be correctly decoded at the receiver [12].

Let $h_{i,j}$ be a complex number corresponding to the channel gain between transmit antenna j and receive antenna i. If at a certain time instant the complex signals $\{x_1, x_2, \ldots, x_{n_T}\}$ are transmitted via n_T transmit antennas, the received signal at antenna i can be expressed as:

$$y_i = \sum_{j=1}^{n_T} h_{i,j} * x_j + n_i \qquad (2.1)$$

Where n_i is a noise term. Combining all receive signals in a vector $\boldsymbol{y}$, Equation (2.1) can be easily expressed in matrix form

$$\boldsymbol{y} = \boldsymbol{H}\boldsymbol{x} + \boldsymbol{n} \qquad (2.2)$$

$\boldsymbol{y}$ is the $n_R \times 1$ receive symbol vector, $\boldsymbol{H}$ is the $n_R \times n_T$ MIMO channel transfer matrix,

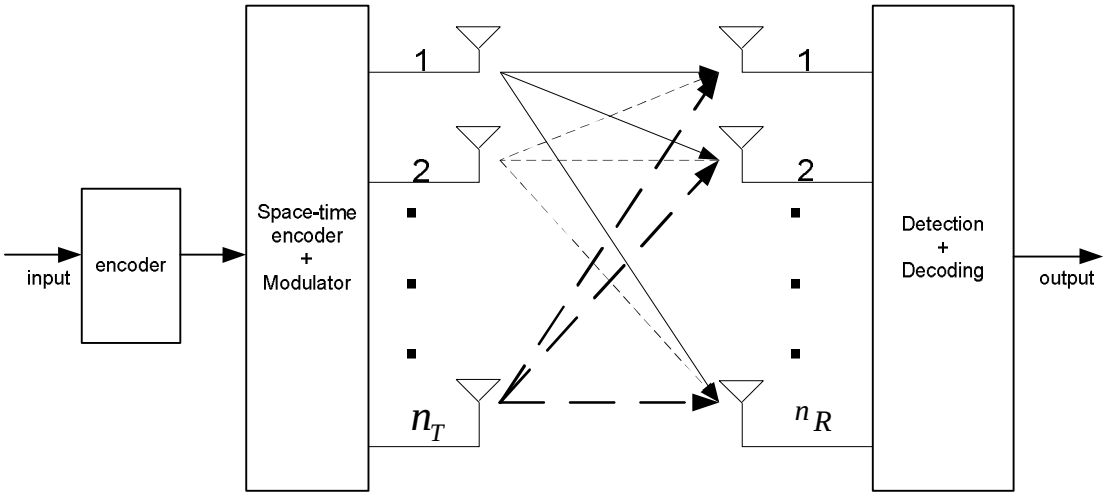

Figure 2.1: General MIMO system with n_T transmit and n_R receive antennas

$$H = \begin{bmatrix} h_{1,1} & \dots & h_{1,n_T} \\ h_{2,1} & \dots & h_{2,n_T} \\ \vdots & \dots & \vdots \\ h_{n_R,1} & \dots & h_{n_R,n_T} \end{bmatrix} \qquad (2.3)$$

$\boldsymbol{x}$ is the n_T × 1 transmit symbol vector and assumed to have Zero mean uncorrelated random variables with variance ${\sigma_x}^2$. The total power of **x** is assumed to be P (independent of the number of transmit antennas). $\boldsymbol{n}$ is the n_R × 1 additive noise vector. Note that the system model implicitly assumes a flat fading MIMO channel, i.e., channel coefficients are constant during the transmission of several symbols. Flat fading, or frequency non-selective fading, applies by definition to systems where the bandwidth of the transmitted signal is much smaller than the coherence bandwidth of the channel. All the frequency components of the transmitted signal undergo the same attenuation and phase shift when propagating through the channel.

In this thesis, we consider the following basic channel model assumption. These models are commonly used in the multiple antenna communications literature and have been proven useful in practice [2, 10, 12, 30].

- **Flat Fading**: We model each wireless link between each pair of transmit and receive antennas as a simple scaling by channel gain h_{ij}. This is valid when the signal bandwidth is narrow enough so that the entire spectrum experiences the same fading coefficient.
- **Rayleigh Fading**: We model the statistics of the random channel coefficient, h_{ij}, using the Rayleigh fading model. This means that they are independent and identically distributed (IID) with zero mean, unit variance, circularly symmetric, complex Gaussian density. It is worth noting that this model is often used because it leads to more tractable theoretical analysis, but it is not entirely accurate. In most environments, the channel coefficients are correlated. The correlation is less when the antennas are well separated and there are a large number of scatters in the environment [2, 12].
- **Channel Knowledge at Receiver**: For most of this thesis, we assume that perfect channel knowledge is available at the receiver but not at the transmitter. Practically speaking, the receiver cannot know the channel perfectly. However, if the channel varies slowly, we can assume that the receiver has sufficient time to get a good estimate of the channel. Again, this assumption is not entirely accurate but makes our problem easier.
- **AWGN at Receiver**: At each receiver, signals received from all transmit antennas are added together, along with an IID additive white (complex) Gaussian noise with zero mean and a variance per dimension of σ^2.

2.2.2 SNR definition

To make a fair performance comparision of systems with, e.g., different coding schemes or modulation schemes in terms of received energy per bit, usually in litrature, the error rate performance is given as function of the bit energy-to-the noise power spectral density ratio E_b/N_o [8, 12, 33]. Whereas for wireless system simulations, in general, the SNR at the receive antenna is used as input parameter. Let E_s/N_o denote the SNR per symbol at the input of the

receiver baseband processinng. Then, clearly, there is a relation between E_b/N_o & E_s/N_o. The relation that is used for the MIMO simulations of this thesis is given below.

The baseband processing of a MIMO transmission system consists of a number of subsequent blocks (see Figure 2.1) that have an influence on the relation between E_b/N_o & E_s/N_o. These blocks are

- The encoder with coding rate R.
- The spatial mapper that maps n_T symbols on n_T transmit antennas.
- The modulation block that maps n_T k bits onto a 2^k-ary modulation scheme.

Now, assume that the communication between the transmitter and receiver is scaled such that the variance of the propagation attenuation is $\sigma_c{}^2$ =1. When $R_b = 1/T_b$ denotes the bit rate and T_s the symbol duration, in general, the relation between E_b/N_o & E_s/N_o is given by

$$\frac{E_b}{N_o} = \frac{E_s}{N_o}\frac{T_b}{T_s} \qquad (2.4)$$

Given this equation, the relation between E_b/N_o & E_s/N_o can be determined per block described above. For an encoder with code rate of R, it can be shown that $T_s = RT_b$ [40]. Thus, substituting this into 2.4 leads to

$$\frac{E_s}{N_o} = R\frac{E_b}{N_o} \qquad (2.5)$$

Sending n_T bits parallel on n_T transmit antennas reflects on the relation between T_s *and* T_b as follows: $T_s = n_T T_b$. Therefore the symbol-energy to noise-density ratio per receive antenna equals

$$\frac{E_s}{N_o} = n_T\frac{E_b}{N_o} \qquad (2.6)$$

The mapping of k bits on M-ary modulation scheme, with M=2^k, leads to the relation

$T_s = kT_b$,

so

$$\frac{E_s}{N_o} = k\,\frac{E_b}{N_o} \tag{2.7}$$

When all the blocks are combined in a serial way, this leads to the following relation

$$\frac{E_s}{N_o} = Rkn_T\,\frac{E_b}{N_o} = \eta_{eff}\,\frac{E_b}{N_o} \tag{2.8}$$

where η_{eff} denotes the spectral efficiency in bits/s/HZ [8], i.e., the ratio between the bit rate and the system bandwidth $B = {}^{1}/_{T_s}$:

$$\frac{E_s}{N_o} = \frac{T_s}{T_b}\,\frac{E_b}{N_o} = \frac{R_b}{B}\frac{E_b}{N_o} = \eta_{eff}\,\frac{\mathrm{E_b}}{\mathrm{N_o}} \tag{2.9}$$

2.3 MIMO Channel Capacity

The commonly used measure of the potential of the channel to transmit data is the capacity [1, 5, 15, 12]. It is the maximum information rate that can be transmitted and received with arbitrarily low probability of error at the receiver within a unit bandwidth. Hence, the capacity is the upper bound of the spectral efficiency achievable in the specific radio channel. For the definition of the capacity, neither the coding scheme nor the modulation is specified. It is the theoretic limit of the transmission rate with a coding block assumed to be infinitely long. Shannon showed that the capacity *C* of the channel with additive white Gaussian noise is limited to [43]:

$$C = \mathrm{B}.\log_2(1 + SNR) \tag{2.10}$$

Where SNR is the signal-to-noise ratio at the receive antenna. Capacity unit is bit/s/Hz. However, in the case of a system with multiple antennas, Shannon's limit should be extended. It was proven [10, 12, 39] that the capacity of the MIMO channel is equal to:

$$C = \log_2 det\left(I_{n_R} + \frac{\rho}{n_T} HH^*\right) \tag{2.11}$$

Where I_{n_R} is $n_R \times n_R$ identity matrix, ρ is the ratio of the total transmit power to the noise power, n_T and n_R are the numbers of Tx and Rx antennas and *H* and H* are the channel transfer matrix

and its transpose conjugate version, respectively. The capacity from Equation (2.11) is sometimes calculated as in [10, 12, 39]:

$$C = \sum_{i=1}^{l} \log_2 \left(1 + \frac{\rho}{n_T} \lambda_i^{\,2}\right) \qquad (2.12)$$

Where l is equal to the rank of the matrix H and $\lambda_1, \lambda_2, \ldots, \lambda_l$ are the singular values of H (nonnegative square roots of the eigenvalues of the matrix HH*). In the case when the transfer functions of the MIMO subchannels are not correlated, e.g. in a richly scattered environment, l is maximal and is equal to min $[n_T, n_R]$. This case will be assumed unless it is stated otherwise. It should be noted that average signal-to-noise ratio at the Rx antennas can be calculated as [12]:

$$SNR = \frac{E_s}{N_o} \cdot \frac{\sum_{i=1}^{n_R} \sum_{j=1}^{n_T} |h_{ij}|^2}{n_T . n_R} \qquad (2.13)$$

Equations (2.11) and (2.12) present the capacity in most popular instance: when the channel transfer matrix is known only at the receiver side. In this case, the capacity of MIMO channel grows proportionally to l [12]: The capacity is the most important measure of the MIMO channel. It determines the possibility of the radio channel for the data transmission.

In the channels with fading, the notion of capacity is not convenient to describe the radio channel. When a deep fade occurs, no data can be transmitted. According to the definition, capacity of such a channel is equal to zero. Thus, instead of the capacity, two other notions are usually used. They are ε-outage capacity and ergodic capacity. The former is suitable when the changes of the channel characteristics are slow and a deep fade could be very long. In this case, the time can be divided into short periods and the capacity can be calculated for each of these periods. Then, the cumulative distributive function is calculated over these values of capacity. On this basis, the ε-outage capacity is defined as a capacity that cannot be achieved ε % of time [1]. So, the capacity of the radio channel is lower than a given value with the probability of ε.

In the channels where the fading is rapid, the expected value of the capacity is usually calculated. Again, the channel can be in a deep fade, but these periods are short and the loss of data can be compensated by the appropriate joint coding and interleaving. This expectation value is called ergodic capacity [41].

2.4 MIMO Space-time Processing

The space-time coding technique is essentially a two-dimensional space and time processing method [8, 33]. While multiple antennas both for transmission and reception are used to improve wireless communication systems capacity and data rate in space-domain, different signals can be transmitted at different time slots using the same antenna at the same time in time-domain. Correlation of time and space is introduced between signals which are transmitted by different antennas so that the receiver antennas can realize diversity reception. Therefore, space-time coding is especially meant for higher coding gain without using more bandwidth which effectively enhances capacity of wireless systems.

MIMO system can be generally divided into Space-Time Coding (STC) and Layered Space-Time Structure (Spatial Multiplexing).

2.4.1 Space-Time Coding (STC)

This approach is performed by adding controlled redundancies in both spatial and temporal domains. These redundancies provide correlations in the transmitted signals to increase the reliability of data transmission. In a multipath environment, MIMO systems employing space-time coding can be used to combat the effect of multipath fading and obtain better error performance. A simple example of space-time code is the Alamouti's Code [42]. This code uses two transmit and two receive antennas to send two symbols over two timeslots. These results in an average transmission rate of one symbol per timeslot and more details on it can be found in [18].

2.4.2 Bell-Labs Layered Space Time Architecture

Foschini and Gans [10] showed that a high bandwidth efficient communication can be achieved with multiple-element antennas over the rich-scattering wireless channel. This technology is called Bell Labs Layered Space Time Architecture (BLAST). BLAST splits a single user’s data

stream into multiple sub-streams and using an array of transmitter antennas simultaneously launches the parallel sub-streams. All sub-streams are transmitted in the same frequency band, so spectrum is used very efficiently. Since the user's data is being sent in parallel over multiple antennas, the effective transmission rate is increased roughly in proportion to the number of transmitter antennas used. There are two main BLAST architectures: diagonal-BLAST (D-BLAST) and vertical-BLAST (V-BLAST).

2.4.2.1 Diagonal-BLAST (D-BLAST)

This architecture is proposed by Foschini [2], which can reach capacities near the Shannon limit. In this architecture, the input data stream is split into n_T substreams [8, 33] by a serial-to-parallel (s/p) converter as shown in Figure 2.3 (b). Then, these substream, also known as layers, are cyclically shifted before transmission. Figure 2.4 (b) illustrates an example of a four-transmit-antenna system with each substream layered diagonally across antennas and time. Note that each symbol transmitted is denoted by $x_i[m]$, where *i* (*i = 1, 2, ..., n_T*) refers to the transmit antenna (layer index) and m (m = 1, 2, 3, ...) refers to the symbol index in each layer & m (m = a, b, c, ...) refers that different symbols transmit at the same time slots. Normally, we leave the letter indexing and use the number indexing only as shown in reference [8].The main reason for transmitting layers from different antennas is to reduce the effect of deep fade by introducing transmit diversity. For instance, if the path gains from one of the transmit antennas are in deep fade, every symbol sent from that particular antenna will be affected and the performance of the system will be significantly degraded. With the cyclic shift feature to distribute the symbols to different antennas, the effect of deep fade is spread out among each layer and it is easier to recover layers with the additional help of an error correcting code. In fact, the role of this cyclic shifting in combating deep fading is similar to the job of interleaving to overcome burst errors. However, this additional feature does come with a price. D-BLAST suffers from high encoding/decoding complexity and also a reduction in the throughput of the system. This reduction is caused by the inefficient use of the first $n_T - 1$ and last $n_T - 1$ time instants as shown in Figure 2.4 (b).

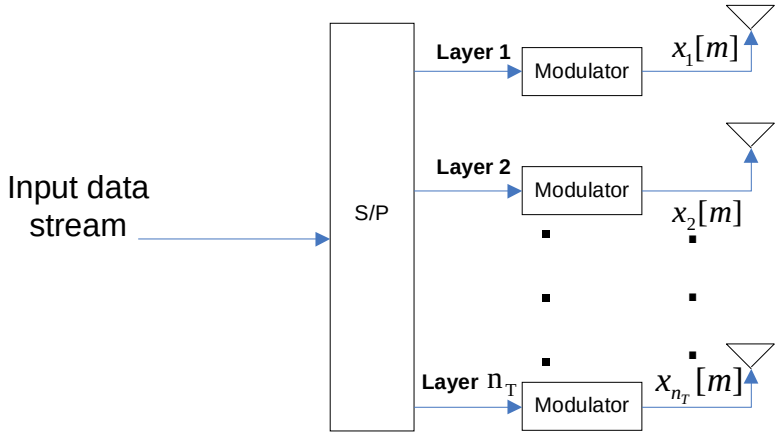

a)

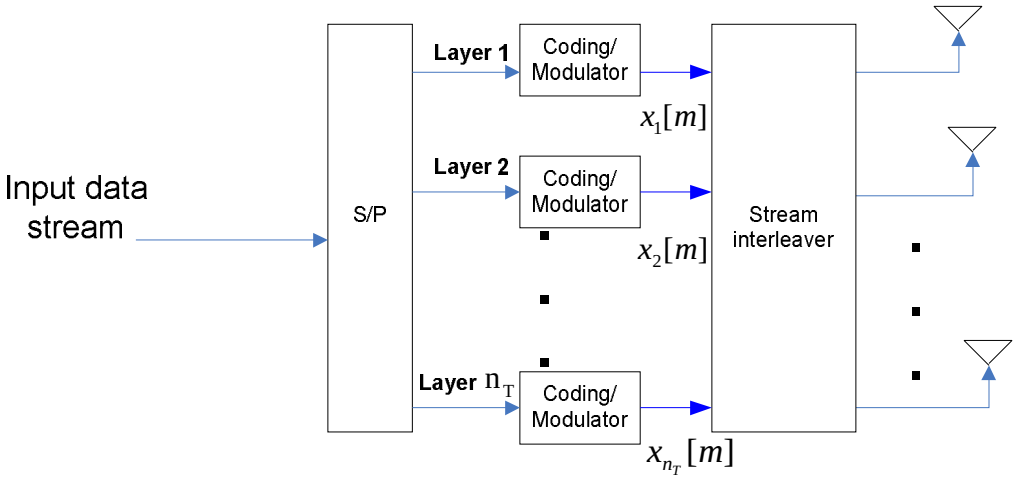

b)

Figure 2.2: a) V-BLAST encoder b) D-BLAST encoder

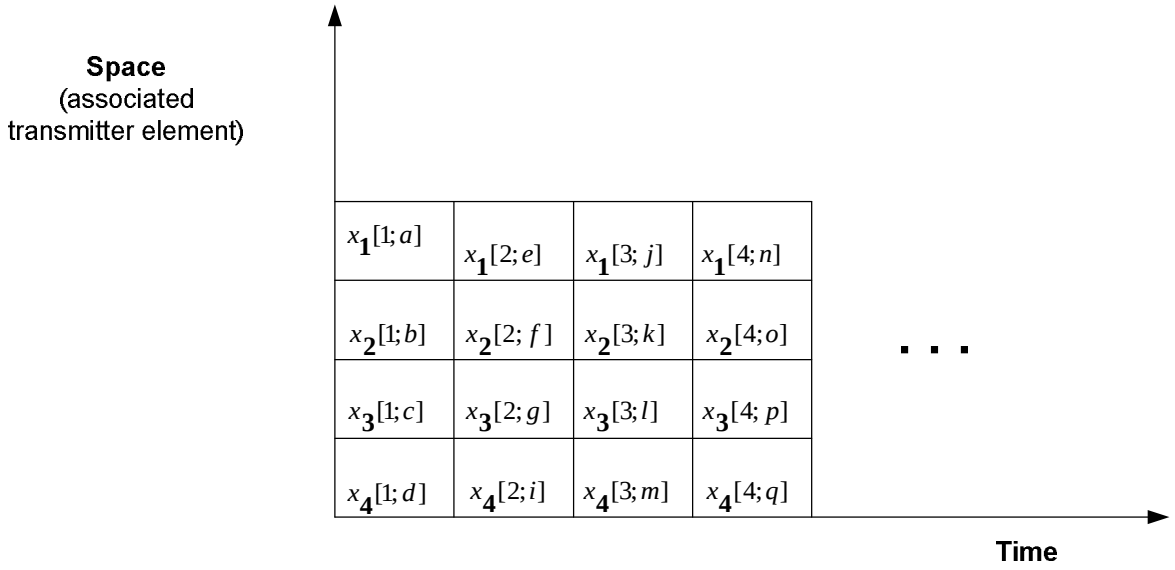

a)

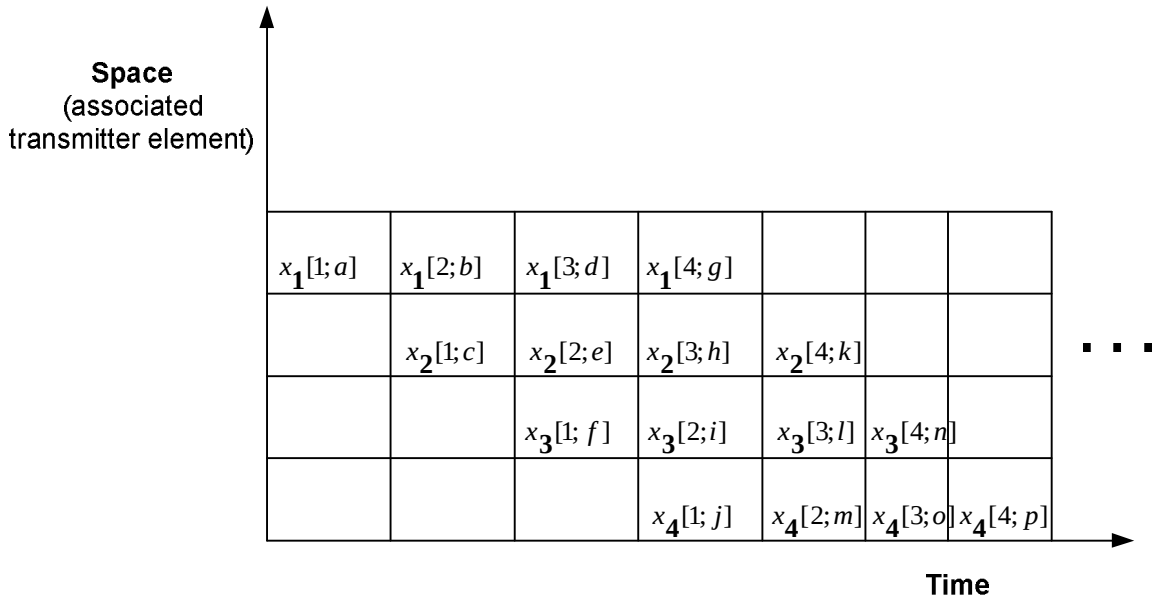

b)

Figure 2.3: Space-time layering (a) V-BLAST (b) D-BLAST

2.4.2.2 Vertical-BLAST (V-BLAST)

As shown in Figure 2.3, the encoder of D-BLAST is very similar to that of V-BLAST. Due to the simple vertical layering in V-BLAST, the encoding and decoding of this scheme is easier [8, 33]; making it the most common form of spatial multiplexing where signals are transmitted from different antenna. In this architecture, the input data stream is split into n_T substreams by a serial-to-parallel (s/p) converter as shown in Figure 2.3 (a). Then, each substream is modulated and transmitted from the corresponding transmit antenna. It is also possible to use error correcting coding in each substream to improve the performance, but uncoded substreams are often assumed in V-BLAST. Figure 2.4 (a) illustrates an example of a four transmit antenna system with vertical layering of the symbols, where each row of symbols is aligned with its corresponding transmit antenna and each column represents the transmitting time instants. As demonstrated, V-BLAST can transmit n_T symbols per channel use.

In this thesis, we chose V-BLAST as our space-time scheme to fully exploit the spatial multiplexing gain in the MIMO channel and due to lower complexities of its receiver implementation. In the next chapter, this V-BLAST architecture and its detection algorithms are described and used.

Chapter 3

Vertical Bell-Labs Layered Space Time Architecture

3.1 Introduction

Two types of BLAST architectures, Diagonal-BLAST and Vertical-BLAST, are mostly discussed in different literatures. The first BLAST proposed in the literature is the D-BLAST architecture [2], which has a diagonal layering space-time coding structure. D-BLAST suffers from boundary wastage at the start and end of each packet, which becomes significant for a small packet size. In addition, the detector of this diagonal approach is very complex and hard to implement. Therefore, a simplified version of BLAST, known as V-BLAST was proposed in [7, 10]. V-BLAST overcomes the limitations of D-BLAST by using independent horizontal layered space-time coding scheme. Note that "vertical" in V-BLAST does not denote the way the parallel data streams are encoded (in general, this is done "horizontally", see Figure 2.4a), but it refers to the way the detection at the receiving end is performed, namely, vertically, i.e., per time instant).

3.2 V-BLAST system

3.2.1 V-BLAST transmitter

Figure 2.3 (a) shows the transmitter in a general V-BLAST system. The input information sequence is first demultiplexed into n_T sub-streams and each of them is subsequently modulated and transmitted from a transmit antenna. The signal processing chain related to an individual sub-stream is referred to as a *layer* [8]. The modulated symbols are arranged into a transmission matrix, denoted by **X**, which consists of n_T rows and L columns, where L is the transmission block length. The m^{th} column of the transmission matrix, denoted by $x[m]$, consists of the modulated symbols $x_1[m]$, $x_2[m]$, . . ., $x_{n_T}[m]$ where m = 1, 2, . . . ,L. At a given time m, the transmitter sends the m^{th} column from the transmission matrix, one symbol from each antenna. That is, a transmission matrix entry $x_i[m]$ is transmitted from antenna i at time m. Vertical structuring refers to transmitting a sequence of matrix columns in the space-time domain.

If the modulator output symbols are denoted by $x_i[m]$, where i represents the layer number and m is the time interval, the transmission matrix, formed from the modulator outputs, denoted by **X**, is given by

$$\mathbf{X}=[\chi_i[m]] \tag{3.1}$$

For example, in a system with three transmit antennas, the transmission matrix **X** is given by

$$\boldsymbol{X} = \begin{bmatrix} x_1[1] & x_1[2] & x_1[3] & \dots \\ x_2[1] & x_2[2] & x_2[3] & \dots \\ x_3[1] & x_3[2] & x_3[3] & \dots \end{bmatrix} \tag{3.2}$$

The sequence $x_1[1], x_1[2], x_1[3], \dots$ is transmitted from antenna 1, the sequence $x_2[1], x_2[2], x_2[3], \dots$ is transmitted from antenna 2 and the sequence $x_3[1], x_3[2], x_3[3], , \dots$ is transmitted from antenna 3.

Note that each column of the transmitted signal matrix **X** corresponds to what is transmitted at one time by the multiple antennas; and each row corresponds to what one antenna transmits over time. When we perform coding across rows of **X**, we refer to it as coding across space. Coding across columns is referred to as coding across time.

3.2.2 V-BLAST receiver

Figure 3.1 is a receiver being used in a general V-BLAST system. All receive antennas receive signals radiated from all transmit antennas; hence there need arise to remove the mixing operation of the channel. As the sub-streams are independently encoded [2, 8], we need to separate the n_T transmitted sub-streams after detection and then decode them separately with their own decoders.

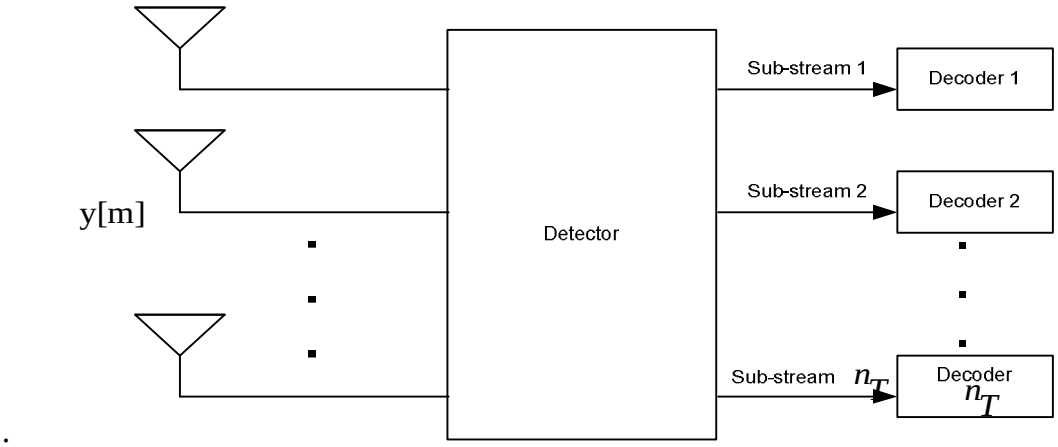

Figure 3.1: Receiver of a general V-BLAST system

Assuming that the receiver is aware of the modulation used, the detection and decoding at the receiver becomes possible through the different V-BLAST signal processing algorithms. In V-BLAST, detection and estimation of the transmitted sub-streams is performed in a vector-by-vector basis, since each vector represents the layer of the V-BLAST coding. Depending on how this is done, there are different methods of detector implementation at receiver side. The most common methods are ML, ZF and MMSE. We assume that the system is quasi-stationary, which implies that the matrix of the channel coefficients remains constant. We also assume that the channel matrix is perfectly known at the receiver side.

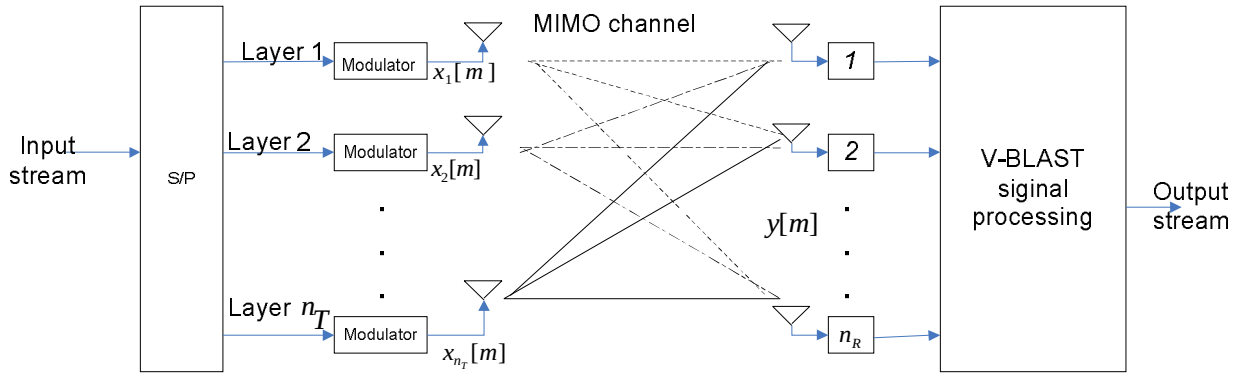

Figure 3.2: V-BLAST system architecture

A high level block diagram of a V-BLAST transceiver system is shown in Fig. 3.2. The signals transmitted from various antennas propagate over independently scattered paths and interfere with each other upon reception at the receiver. This interference can be represented by the following matrix operation at a given time instant *m*.

$$y[m] = Hx[m] + n[m] \qquad (3.3)$$

Where $y[m]$ is an n_R-component column matrix of the received signals across the n_R receive antennas. The matrix channel transfer function is H (n_R x n_T), where h_{ij} is the (complex) transfer function from transmitter j to receiver i, and $n_T \leq n_R$. $x[m]$ is the m^{th} column in the transmission matrix $\boldsymbol{X}$ and $n[m]$ is an n_R-component column matrix of the AWGN noise signals from the receive antennas, where the noise variance per receive antenna is denoted by σ^2.

3.3 V-BLAST detectors

3.3.1 Linear detectors

3.3.1.1 Zero-Forcing detector (Geometric Derivation)

When the transmitter does know the channel, the singular value decomposition (SVD) architecture enables the transmitter to send parallel data streams through the channel so that they arrive orthogonally at the receiver without interference between the streams. This is achieved by pre-rotating the data so that the parallel streams can be sent along the eigenmodes of the channel [1]. When the transmitter does not know the channel, this is not possible. For example, if the transmitter sends independent data on each of the transmit antennas (a parallel data stream), then after passing through the MIMO channel, they all arrive cross-coupled at the receiver. It is necessary that the receiver be able to separate the data streams efficiently enough so that the resulting performance has full degrees of freedom. To simplify notations, we will introduce the time-invariant case where the channel matrix is fixed. We can write the received vector at time instant *m* as

$$y[m] = \sum_{i=1}^{n_T} h_i[m] x_i[m] + n[m] \qquad (3.4)$$

Where $\mathbf{h_1}$, $\boldsymbol{h_2}$, ..., $\boldsymbol{h_{n_T}}$ are the columns of H and the data sub-streams transmitted on the antennas, $\{x_i[m]\}$ on the i^{th} antenna, are all independent. Focusing on the k^{th} data sub-stream, we can rewrite (3.4):

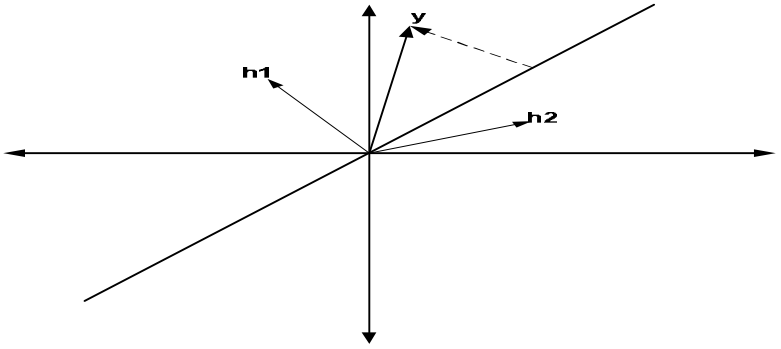

Figure 3.3: A projection operation: **y** is projected onto the subspace orthogonal to **h1** to demodulate sub-stream 2

$$y[m] = h_k\, x_k[m] + \sum_{i \neq k}^{n_T} h_i\, x_i[m] + n[m] \qquad (3.5)$$

Unlike SIMO point-to-point channel, we see that the k^{th} data stream faces an extra source of interference, that from the other data streams. One idea that can be used to remove this inter stream interference is to project the received signal **y** onto the subspace orthogonal to the one spanned by the vectors $\boldsymbol{h_1}, \boldsymbol{h_2}, \dots, \boldsymbol{h_{k-1}}, \boldsymbol{h_{k+1}}, \dots, \boldsymbol{h_{n_T}}$ (denoted henceforth by V_k). Supposing that the dimension of V_k is d_k. Projection is a linear operation and we can represent it by a $V_k x n_R$ matrix $\mathbf{Q_k}$, the rows of $\mathbf{Q_k}$ form an orthonormal basis of V_k; they are all orthogonal to $\boldsymbol{h_1}, \boldsymbol{h_2}, \dots, \boldsymbol{h_{k-1}}, \boldsymbol{h_{k+1}}, \dots, \boldsymbol{h_{n_T}}$. The vector $\mathbf{Q_k v}$ should be interpreted as the projection of the vector **v** onto V_k, but expressed in terms of the coordinates defined by the basis of V_k. A pictorial depiction of this projection operation is in Figure 3.3.

Now, the inter-stream interference "nulling" is successful (that is, the resulting projection of $\boldsymbol{h_k}$ is a non-zero vector) if the k^{th} data stream "spatial signature" $\boldsymbol{h_k}$ is not a linear combination of the spatial signatures of the other data streams. In other words, if there are more data streams than the dimension of the received signal (i.e., $n_T > n_R$), then the Zero-Forcing detector operation

will not be successful, even for a full rank H. Hence, we should choose the number of data streams to be no more than n_R [1]. Physically, this corresponds to using only a subset of the transmit antennas and for notational convenience we will count only the transmit antennas that are used, by just making the assumption $n_T \leq n_R$ in the Zero-Forcing detector henceforth. Using a matched filter to demodulate the k^{th} stream, after matched filtering $\boldsymbol{Q_k h_k}$, the output has SNR [1] is

$$\frac{P_k \|Q_k h_k\|^2}{N_o} \qquad (3.6)$$

Where P_k is the power allocated to sub-stream k.

The combination of the projection operation and the matched filtering is called *Zero-Forcing* receiver, which is also known as *interference nulling* or *decorrelator*. The Zero-Forcing detector is a linear filter since projection and matched filtering are both linear operations. Consider a projection of h_k onto subspace V_k, the filter $\boldsymbol{c_k^*}$ is given by

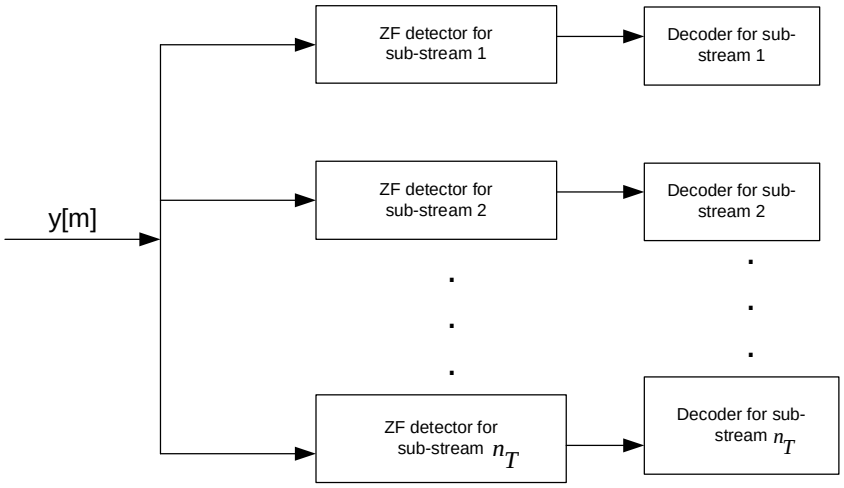

Figure 3.4: A bank of Zero-Forcing detectors, each estimating the parallel data sub-streams

$$\boldsymbol{c_k^*} = (\boldsymbol{Q_k h_k})^* \boldsymbol{Q_k} \qquad (3.7)$$

which is the projection of $\boldsymbol{h_k}$ onto the subspace V_k, expressed in terms of the original coordinates. Since the matched filter maximizes the output SNR, the Zero-Forcing detector can also be interpreted as a linear filter that maximizes the output SNR, but with a constraint that the

filter nulls out the interference from all the other streams. Intuitively, we are projecting the received signal in the direction within V_k that is closest to $\boldsymbol{h_k}$.

Only the k^{th} sub-stream has been in focus so far. We can now decorrelate each of the sub-streams separately, as illustrated in Figure 3.4. We have described the Zero-Forcing detector geometrically; however there is a simple explicit formula for the entire bank of Zero-Forcing detectors [1]: the Zero-Forcing detector for the k^{th} sub-stream is the k^{th} column of the pseudo-inverse w of the matrix H, defined by

$$w = (H^*H)^{-1}H^* \qquad (3.8)$$

3.3.1.2 Minimum mean square error (MMSE) detector

The MMSE detector suppresses both the interference and noise components, whereas the ZF detector removes only the interference components. In the MMSE detection algorithm, the expected value of the mean square error between the transmitted vector **x** and a linear combination of the received vector $w^H y$ is minimized [8].

$$min\ E\{(x - w^H y)^2\} \qquad (3.9)$$

Where w is an $n_R \times n_T$ matrix of linear combination coefficients given by [22]

$$w^H = \left[H^H H + \sigma^2 I_{n_T}\right]^{-1} H^H \qquad (3.10)$$

σ^2 is the noise variance and I_{n_T} is an $n_T \times n_T$ identity matrix. The decision statistics for the sub-stream sent from antenna *i* at time instant *m* is obtained as

$$y_i[m] = w_i^H y \qquad (3.11)$$

Where w_i^H is the i^{th} row of w^H consisting of n_R components. The estimate of the sub-stream sent by the antenna i, is denoted by

$$\tilde{x}_i[m] = q(y_i[m]) \qquad (3.12)$$

Where *q(x)* denotes the hard decision or slicing operation on *x*.

In an algorithm with interference suppression only, the detector calculates the hard decision estimates by using (3.11) and (3.12) for all sub-streams and a bank of MMSE detectors, each estimating a parallel data sub-stream is shown in figure 3.5 below.

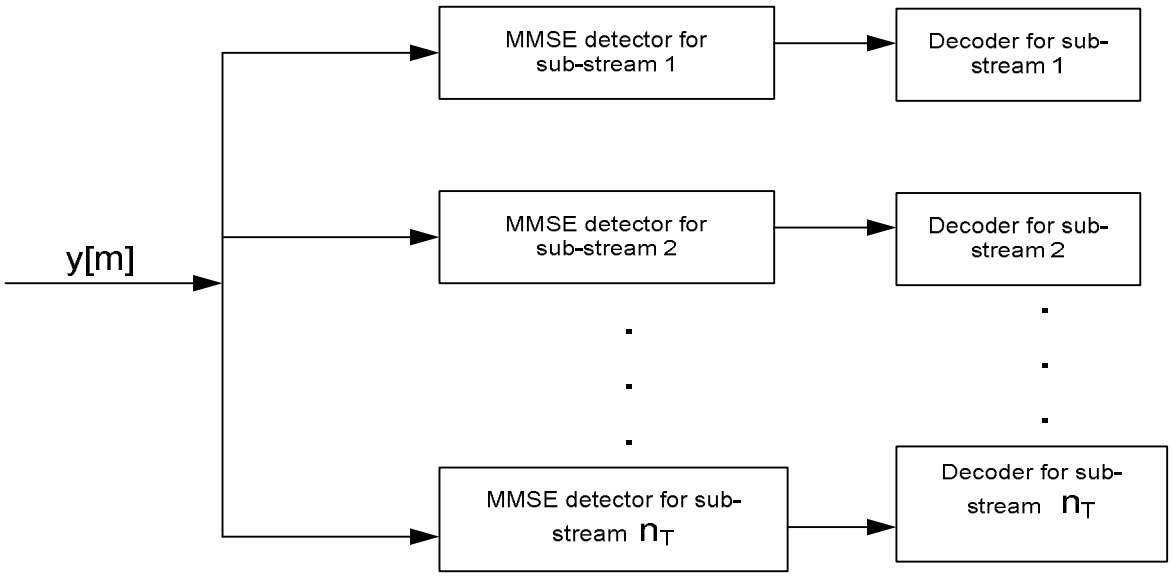

Figure 3.5: A bank of MMSE detectors, each estimating a parallel data sub-streams

3.3.2 Non-linear detectors

3.3.2.1 Successive interference cancellation

Zero-Forcing with SIC

So far, we have just considered a bank of *separate* filters to estimate the data streams. However, the result of one of the filters could be used to aid the operation of the others. Thus, we can use the *successive cancellation* strategy: once a data stream is successfully recovered, we can subtract it off from the received vector and reduce the burden on the receivers of the remaining data streams. With this motivation, we make the following modification to the bank of separate receiver structures in Figure 3.4. We use the first Zero-Forcing detector to decode the data stream $x_1[m]$ and then subtract off this decoded stream from the received vector.

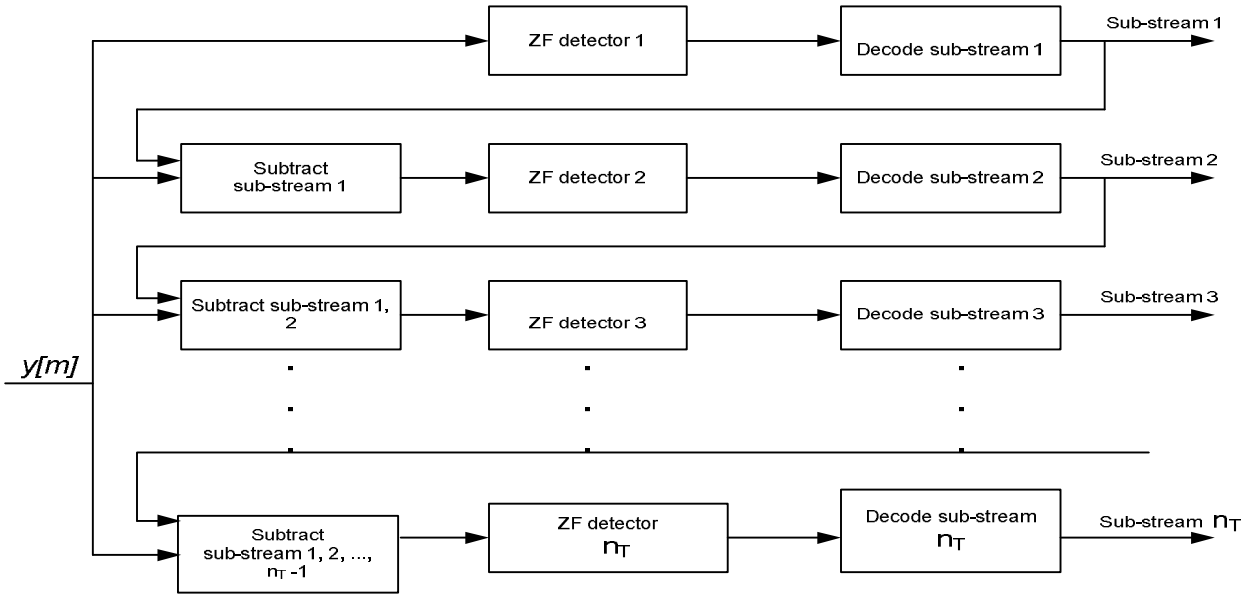

Figure 3.6: SIC Zero-Forcing detector: A bank of Zero-Forcing detectors with successive cancellation of sub-streams

Assuming the first stream is successfully decoded, and then the second Zero-Forcing detector only needs to deal with streams $x_3, x_4, \dots, x_{n_T}$ as interference, since x_1 has been correctly subtracted off. Thus, the second Zero-Forcing detector projects onto a subspace which is orthogonal to that spanned by $\boldsymbol{h_3}, \boldsymbol{h_4}., \dots, \boldsymbol{h_{n_T}}$. This process is continued until the final Zero-Forcing detector does not have to deal with any interference from the other data streams (assuming successful subtraction in each preceding stage).This Zero-Forcing with Successive Interference Cancellation detector architecture (ZF-SIC) is illustrated in Figure 3.6.

One problem with this SIC receiver structure is *error propagation*: an error in decoding the k^{th} data stream means that the subtracted signal is incorrect and this error propagates to all the streams further down, $k + 1, \dots, n_T$. A careful analysis of the performance of this scheme is complicated, but can be made easier if we take the data streams to be well coded and the block length to be very large, so that streams are successfully cancelled with very high probability. With this assumption the k^{th} data stream sees only down-stream interference, i.e., from the streams $k + 1, \dots, n_T$. Thus, the corresponding projection operation (denoted by $\widetilde{\boldsymbol{Q}}_{\boldsymbol{K}}$) is onto a

higher dimensional subspace (one orthogonal to that spanned by $\boldsymbol{h_{k+1}, \ldots, h_{n_T}}$, as opposed to being orthogonal to the span of $\boldsymbol{h_1, h_2, \ldots, h_{k-1}, h_{k+1}, \ldots, h_{n_T}}$). As in the calculation of the previous section, the SNR of the k^{th} data stream [1] is

$$\frac{P_k \|\tilde{Q}_K h_k\|^2}{N_O} \qquad (3.13)$$

Minimum mean square error (MMSE) with SIC

We have considered a bank of separate filters to estimate the data streams in figure 3.5. However, we can use the result of one filter to help the operation of other filters similar to the zero forcing SIC detectors. Once a data stream is successfully recovered, we can subtract it from the received vector and reduce the burden on the receiver of the remaining data streams.

After the nulling operation, assuming that $\tilde{x}_i = x_i$, we cancel x_i from y_i and generate a modified received signal vector y_{i+1} for i= 1, 2, ..., n_T. Figure 3.7 shows a bank of MMSE detectors with successive cancellation of sub-streams.

$$y_{i+1} = y_i - \tilde{x}_i w_i^H \qquad (3.14)$$

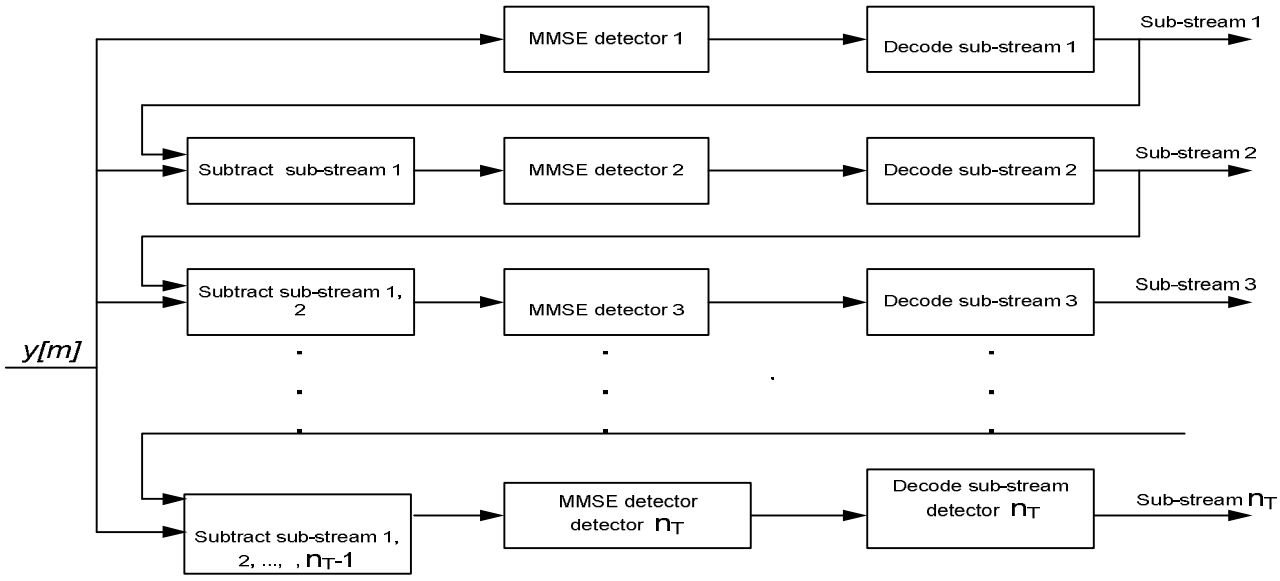

Figure 3.7: SIC MMSE detector: A bank of MMSE detectors with successive cancellation of sub-streams

3.3.2.2 Ordered Successive interference cancellation

Zero-Forcing SIC with ordering

Consider the problem of the error propagation we discussed in Section 3.3.2.1. In a real communication system, it is impossible to cancel the streams perfectly, thus the error propagation is unavoidable. Furthermore, the error propagation has a negative impact on the error rate performance of the receiver. Our goal is trying to make this error propagation as small as possible.

In order to combat the error propagation, we need to utilize an ordering strategy in our V-BLAST system. Ordering is a method of easing the error propagation by sorting the order of the streams being detected. Streams with higher post detection SNRs may have lower error probabilities, thus processing these streams at earlier stages lead to less errors.

Each signal is an interferer to the rest of the signals. The best signal stream in terms of SNR is selected for detection and is also removed from the remaining signals. This way, the remaining signals have one interferer less. Optimal combining is repeated until all signals are detected.

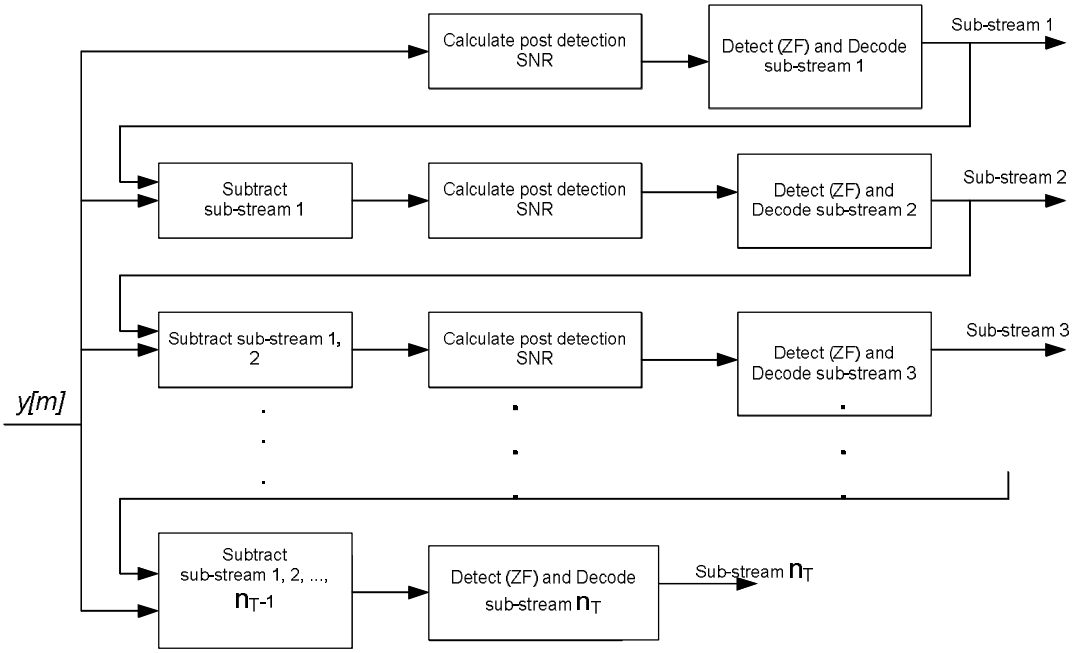

Figure 3.8: SIC ordering Zero-Forcing: A SIC detector with ordering strategy

Three consecutive phases take place for SIC ordering Zero-Forcing in [33]:

- Linear interference suppression
- Interference cancellation of the substreams detected
- Reordering of the detection process through SNR post-detection

This operation is realized in three steps:

$$\begin{aligned} w_{k_i} &= (G_i)_{k_i} \\ z_{k_i} &= w_{k_i}^T . y_i \\ \tilde{x}_{k_i} &= q(z_{k_i}) \end{aligned} \qquad (3.15)$$

The first step consist on finding the zero-forcing vector w_{k_i} that satisfies:

$$w_i^T . (H)_j = \begin{cases} 0 & j>i \\ 1 & j=i \end{cases} \qquad (3.16)$$

In Equation 3.16, $(H)_j$ represents the j^{th} column of H which is a vector composed of all the channel coefficients produced from transmit antenna j. It turns out that the condition of Equation 3.16 is realized by taking w_i to be the equivalent j^{th} column from the Moore-Penrose pseudo-inverse [33, 49]. Hence, the algorithm finds the zero-forcing vector w_{k_i} through consecutively calculating the Moore-Penrose pseudo-inverse. In the first line of Equation 3.15, i is the iteration number, k_i is the index of the transmit antenna whose substream is detected during iteration i and G_i is the Moore-Penrose pseudo-inverse at iteration stage i. With w_{k_i}, the statistic decision z_{k_i} is obtained from the received vector y_{k_i} at stage i, and is quantized (represented by the operator q(.) in order to obtain the k_i^{th} detected substream.

The interference of the detected substream is cancelled in the second step of the algorithm by removing its interference from the received signal:

$$\begin{aligned} y_{i+1} &= y_i - \tilde{x}_{k_i} . (H)_{k_i} \\ G_{i+1} &= H_{k_i}^{\pm} \end{aligned} \qquad (3.17)$$

A new received vector y_{i+1} is formed by removing from y_i the estimated transmit signal of the detected substream. The Moore-Penrose pseudo-inverse (represented by the + sign as

superscript) is recalculated from the previous stage transfer matrix after annulling its k_i^{th} row. The operations realized in Equation 3.17 can be seen as redefining a new system where the antenna that used to transmit the previous detected substream is extinguished. This is achieved by removing the signal produced by the detected substream and by annulling the channel coefficients related to the estimated substream's antenna.

The last step of the process is charged to select the optimum order for decoding. In other words, the layers are rearranged in the process in order to minimize the probability of error. This means finding an index k_i of stage i. The method proposed in the algorithm is to select the antenna with the best post-detection SNR. The post-detection SNR of each transmit antenna j is the absolute value of the j^{th} column of the Moore-Penrose pseudo-inverse G_i at stage i. If S is the optimum ordering and $S = \{k_1, k_2, \dots k_{n_T}\}$, the search for the best SNR post-detection at stage i is performed for the set $\{k_i, k_2, \dots k_{n_T}\}$, since the substreams transmitted from antennas k_1 to k_i already have been detected in previous stages. The best post-detection SNR is the minimum absolute value calculated:

$$k_i = \underset{j \in S, j \notin \{k_1, k_2, \dots k_{i-1}\}}{arg\,min} \left\| (G_i)_j \right\|^2 \qquad (3.18)$$

The generalized algorithm is composed of two phases, an initialization and a recursive phase [33]. The initialization phase consists of calculating the Moore-Penrose pseudo-inverse:

$$G_1 = H^+ = W_{ZF} = (H^H H)^{-1} H^H \qquad (3.19)$$

$$i = 1$$

The recursive phase is composed of the previously described steps:

$$k_i = \underset{j \in S, j \notin \{k_1, k_2, \dots k_{i-1}\}}{arg\,min} \left\| (G_i)_j \right\|^2$$

$$w_{k_i} = (G_i)_{k_i}$$

$$z_{k_i} = w_{k_i}^T y_i$$

$$\hat{x}_{k_i} = Q(z_{k_i}) \qquad (3.20)$$

$$y_{i+1} = y_i - \hat{x}_{k_i}(H)_{k_i}$$

$$G_{i+1} = H_{k_i}^{\pm}$$

$$i = i + 1$$

Instead of processing the substreams according to the order in Figure 3.7, we calculate the post detection SNR of each substream; put the substreams in order from the highest SNR to the lowest SNR. Then we select the substream with the highest post detection SNR as the substream No.1. We apply this stream with its corresponding Zero-Forcing detector, decode and subtract it from the received vector. After subtraction, we will have a new MIMO system with $n_T - 1$ transmitting substreams and n_R receiving antennas. Now we calculate the post detection SNR for the new $n_T - 1x\, n_R$ system, select the substream with the highest SNR as the substream No.2, continue the above steps until all the transmitted substreams are decoded. An illustration of the SIC ordering ZF detector is shown in Figure 3.8.

MMSE SIC with ordering

When the cancellation of the detected substream is employed, the order in which the components of $\boldsymbol{x}$ are detected is important to the overall system performance. In the ordering strategy, we choose the data substream with the highest post detection SNR every time; this makes sure that the number of the errors being propagated to the next stage is the smallest.

Instead of processing the substreams according to the order in Figure 3.7, we calculate the post detection SNR of each substream. Then we put the substreams in order from the highest SNR to the lowest SNR and apply this substream with its corresponding MMSE detector, decode and subtract it from the received vector similar to the zero-forcing algorithm. An illustration of the SIC ordering MMSE detector is shown in Figure 3.9.

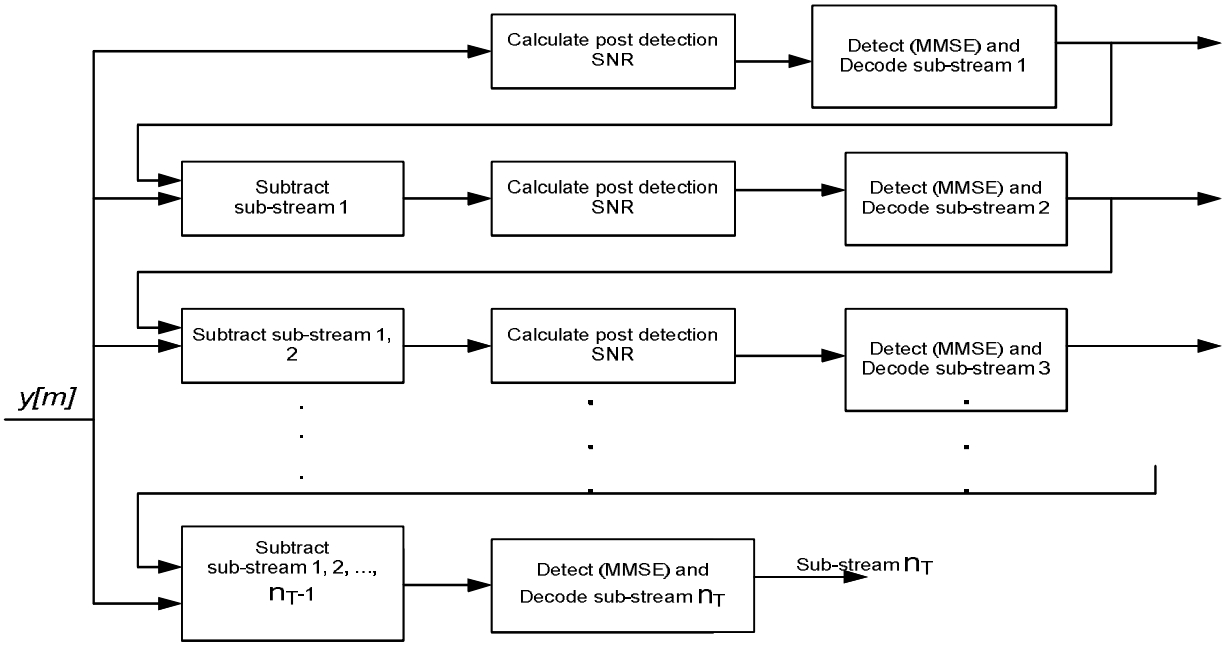

Figure 3.9 SIC ordering MMSE: A SIC detector with ordering strategy

The mathematical description for the minimum mean square error detection algorithm which is a recursive procedure with ordering strategy is shown below [8] & [33].

Initialization :

$$G_1 = W_{MMSE} = \left(H^H H + \sigma^2 I_{n_T}\right)^{-1} H^H$$

$$i = 1 \qquad (21)$$

$$k_1 = arg\,min \left\|(G_i)_j\right\|^2$$

Recursion*:*

$$w_{k_i} = (G_i)_{k_i}$$

$$z_{k_i} = w_{k_i}^T y_i$$

$$\hat{x}_{k_i} = Q\left(z_{k_i}\right) \qquad (3.22)$$

$$y_{i+1} = y_i - \hat{x}_{k_i}(H)_{k_i}$$

$$G_{i+1} = \left(H_i^H H_i + \sigma^2 I_{n_T}\right)^{-1} H_i^H$$

$$k_{i+1} = \underset{j \notin \{k_1, k_2, \ldots k_{i-1}\}}{arg\,min} \|(G_i)_j\|^2$$

$$i = i + 1$$

3.3.2.3 Maximum Likelihood Detection (MLD)

The ML receiver performs optimum vector decoding and is optimal in the sense of minimizing the error probability. ML receiver is a method that compares the received signals with all possible transmitted signal vector which is modified by channel matrix H and estimates transmit symbol vector x over the set χ^N according to the Maximum Likelihood principle [37], which is shown as below and corresponds to the minimum Euclidean distance rule:

$$\hat{\boldsymbol{x}} = arg \underset{\mathrm{x} \in \chi^{\mathrm{N}}}{\min} \|\boldsymbol{y} - \boldsymbol{H}\boldsymbol{x}\|^2 \qquad (3.23)$$

Where the minimization is performed over all possible transmitted symbol vectors χ^N. Although ML detection offers optimal error performance, it suffers from complexity issues. It has exponential complexity in the sense that the receiver has to consider $|A|^{n_T}$ possible symbols for an n_T transmitter antenna system with A is the modulation constellation.

3.4 Complexity of detectors

Before we determine the complexity of the V-BLAST detection algorithms, we introduce a number of general rules about the complexity of a matrix multiplication, the conversion from complex complexity figures to real complexity figures, the complexity of a slicer, and the complexity of finding a minimun value from a set of values.

The complexity of a matrix product is determined as follows. Suppose two matrices **A** and **B** (real or complex) with dimesions **C x D** and **D x E** are multiplied, then the $(i, l)^{th}$ element of the resulting matrix is given by [49]

$$a^i b_l = \sum_{k=1}^{D} a_{lk} b_{kl} \quad (3.24)$$

Where a^i represents the i^{th} row of matrix **A**, b_l denotes the l^{th} column of **B** and a_{lk} *and* b_{kl} stand for the k^{th} element of this row and column, respectively. Thus, in order to obtain one element of the resulting matrix, **D-1** additions and **D** multiplications need to be performed. The resulting matrix **C x E** is dimensional and, therefore, a total of **C.(D-1).E** additions and **C.D.E** multiplications are needed to multiply the two matrices **A** and **B**.

To write complex additions and complex multiplications in terms of real additions and real multiplications, it is easily verified that one complex addition consists of two real additions; the real and the imaginary part of the two complex numbers are added. Furthermore, a complex multiplication can be rewritten in the following form [45].

$$(a + jb)(c + jd) = (ac - bd) + j(bc + ad) \quad (3.25)$$

This multiplication consists of 4 real multiplications (ac, bd, bc *and* ad) and 2 real additions ($ac - bd$ *and* $bc + ad$). A subtraction is counted as an addition and the addition before j does not count because the real and imaginary part are stored separately.

The complexity of a slicer is minimal in terms of additions and/or multiplications. For an M-psk constellation scheme, the phase range $[-\pi, \pi]$ is divided in M equal parts. In such a regular structure, we can recursively search in which half of the (remaining) range the phase of the estimated symbol best fits. This results in a complexity equivalent to $\log_2 M$ comparisions [40]. For an M-QAM constellation diagram, we can split the real and imaginary part. Each of these parts is regularly divided in $\sqrt{M}$ slicing ranges. Also, in this case, we can recursively search in which half of the (remaining) range the real or imaginary part of the estimated symbol best fits, and the complexity is equal to $\log_2 \sqrt{M}$ comparisions for the real and for the imaginary part, or 2. $\log_2 \sqrt{M} = \log_2 M$ comparisions in total. It is reasonable to assume that a comparision is as complex as a real addition and, therefore, the slicing of n_T –dimensional vector requires at most $n_T \cdot \log_2 M$ real additions.

In order to find the minimum of N numbers, the easiest thing to do is start with the first two elements, subtract the second number from the first, and compare the result with zero. If the result is larger than zero, the second number is smallest, otherwise the first number is the

smallest, etc. Obviously, finding the minimum between two real numbers has the complexity of one real additions. As a result, determining the minimum N values has a complexity of N-1 real additions.

The computational complexities of the V-BLAST detectors depend on the type of detection algorithm used and the general rules given above. For instance, the complexity of the zero-forcing detection algorithm is based on calculation of the pseudo-inverse of the channel transfer matrix H. Because it is assumed that the MIMO channel is quasi-static, i.e., H is constant during the packet transmission. Therefore, the pseudo-inverse of H needs to be calculated only once per packet. For determining the complexity of the pseudo-inverse, we will use the equality that can be deduced from (3.8) and given by

$$W = (H^H H)^{-1} H^H \qquad (3.26)$$

The dimensions of W, H^H and H are n_T x $n_{R,}$, n_T x n_R and n_R x n_T respectively. To find the pseudo-inverse of H, we first need to determine the complexity of the matrix product $H^H H$. By using the general rules given above, the complexity of the matrix product $H^H H$ yields $n_T^2\,(n_R - 1)$ complex additions and $n_T^2\, n_R$ complex multiplications. The result is a square matrix with dimensions n_T x n_T

From this square matrix $H^H H$, the inverse needs to be determined. In [40, 45] it is shown that the direct inversion of a given square matrix A (with dimensions NxN) has a complexity in the order of N^3 additions and N^3 multiplications in total. So, inverting $H^H H$ has acomplexity of N^3 complex additions and N^3 complex multiplications.

Finally, the inverse of $H^H H$ is multiplied by H^H. The complexity of this last multiplication is equal to $n_T.(n_R - 1)$ complex additions and $n_T^2\, n_R$ complex multiplications. This leads to a total complexity of $4n_T^3 + n_T^2.(8n_R - 2) - 2n_T n_R$ real additions and $4n_T^3 + 8n_T^2 n_R$ real multiplications.

During the slicing step the matrix vector multiplication is given by

$$\tilde{x} = W.x \qquad (3.27)$$

The complexity of this product is equal to $n_T^2\,(n_R - 1)$ complex additions and $n_T n_R$ complex multiplication. From the general rules for slicing given above, the complexity of slicing n_T M-

ary constellation points equals to $n_T.\log_2 M$ real additions. In general, the complexity of the ZF algorithm during the estimation and slicing operation per transmitted vector x is equal to $(2n_T n_R + 2n_T(n_R - 1) + n_T.\log_2 M)$ real additions and $4n_T n_R$ real multiplications. When N_S vectors are transmitted within a packet, these numbers must be multiplied by N_S to obtain the total complexity. Finally, the total complexity of the ZF algorithm during the finding of pseudo-inverse of the channel transfer matrix H, the estimation and slicing operation is equal to $4n_T^3 + n_T^2.(8n_R - 2) - 2n_T n_R + N_S.(2n_T n_R + 2n_T(n_R - 1) + n_T.\log_2 M)$.

As far as the complexity of the other detection methods is concerned [36, 40, 44] has given detailed analysis and the summarized complexity of the different detectors is given below in table form & their simulation outputs are shown in Figures 3.10 and 3.11. For consistent comparison, the complex operations are converted to real operation equivalents.

Table 1: Computational complexity of detectors in terms of additions and multiplications

Detector	Total No. of real additions	Total No. of real multiplications
ZF	$4n_T^3 + n_T^2.(8n_R - 2) - 2n_T n_R + N_S.(2n_T n_R + 2n_T(n_R - 1) + n_T.\log_2 M)$	$4n_T^3 + 8n_T^2 n_R + N_S.(4n_T n_R)$
MMSE	$4n_T^3 + n_T^2.(8n_R - 2) - 2n_T n_R + n_T + N_S.(2n_T n_R + 2n_T(n_R - 1) + n_T.\log_2 M)$	$4n_T^3 + 8n_T^2 n_R + N_S.(4n_T n_R)$
ZF-OSIC	$n_T.(3n_T^3 + 4.n_T^2(1 + 2n_R) + 3n_T(1 + 3n_R) + n_R - 1).\frac{1}{3} + N_S.(2n_T(4n_R - 1) + n_T.\log_2 M)$	$n_T^2.(n_T + 1)^2 + 8n_T n_R.\frac{(n_T + 1)(2n_T + 1)}{6} + N_S.(8n_T n_R)$
MMSE-OSIC	$n_T.(3n_T^3 + 4.n_T^2(1 + 2n_R) + 3n_T(1 + 3n_R) + n_T + n_R - 1).\frac{1}{3} + N_S.(2n_T(4n_R - 1) + n_T.\log_2 M)$	$n_T^2.(n_T + 1)^2 + 8n_T n_R.\frac{(n_T + 1)(2n_T + 1)}{6} + N_S.(8n_T n_R)$
ML	$N_S.((2M^2 n_R \frac{M^{n_T-1}-1}{M-1} + 2Mn_T n_R + 4n_R N_S - 1)$	$N_S.(4Mn_T n_R + 2n_R N_S)$

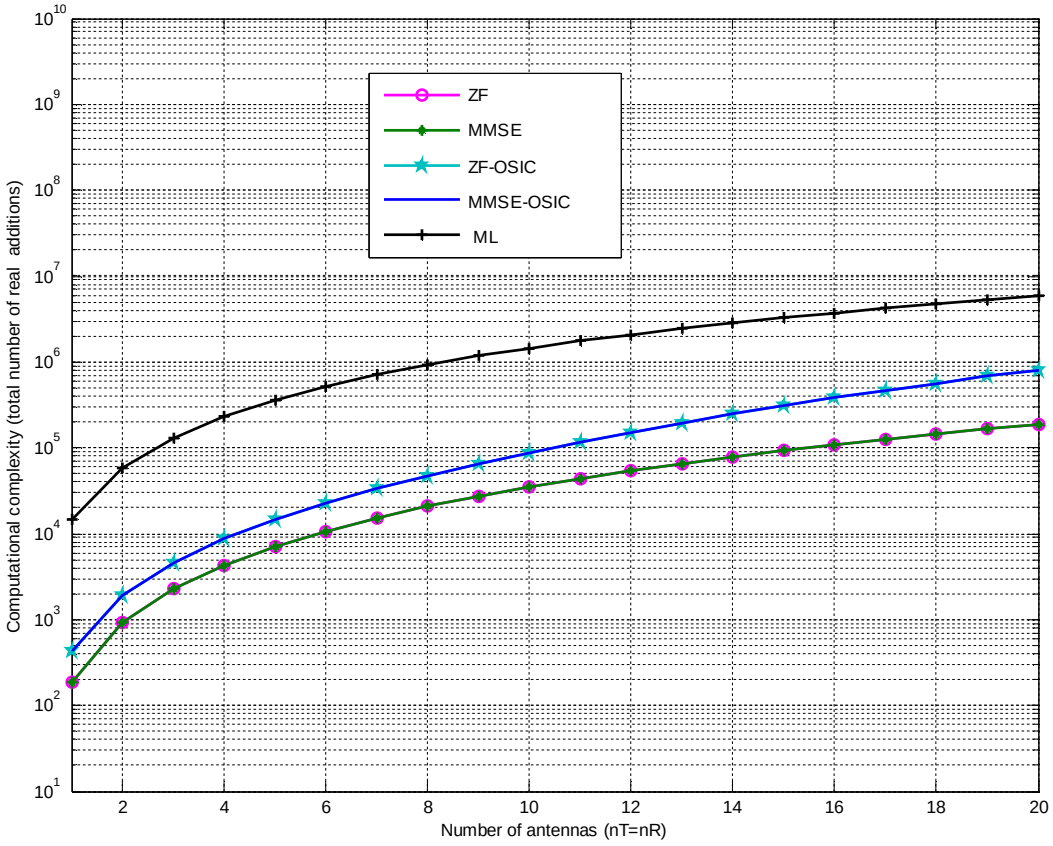

Figure 3.10: Computational complexity of different V-BLAST detectors for BPSK modulation

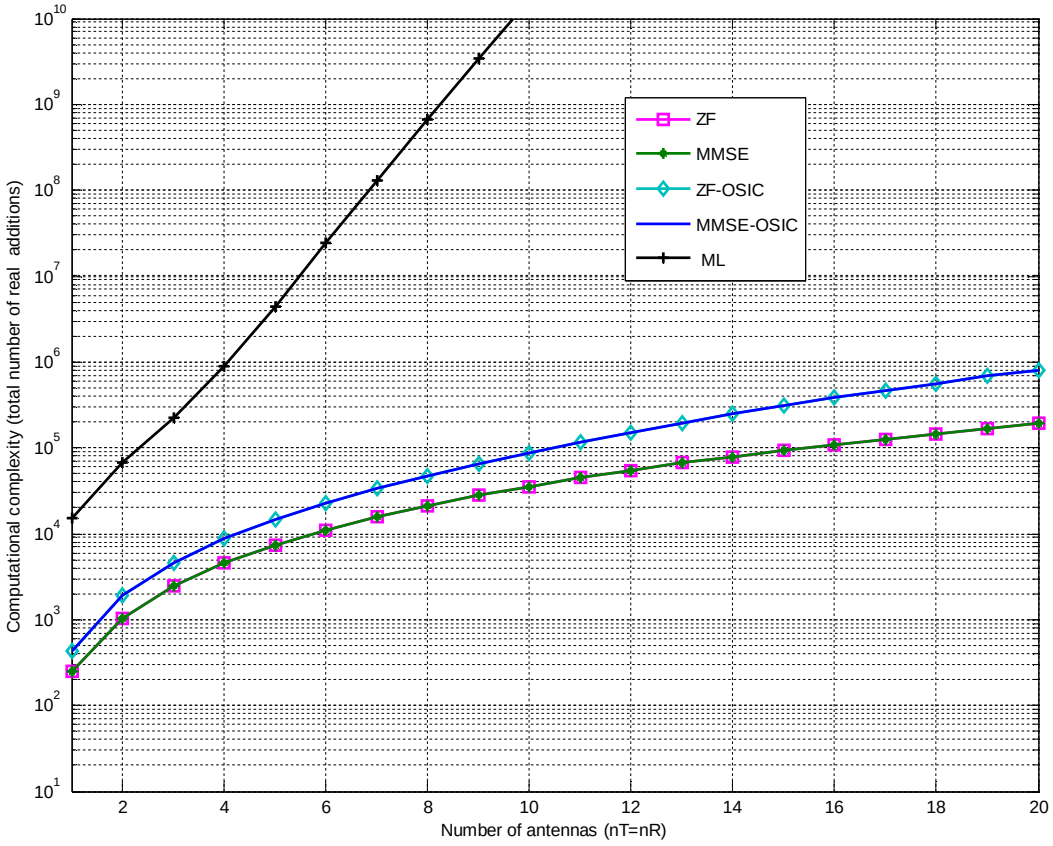

Figure 3.11: Computational complexity of different V-BLAST detectors for QAM modulation

3.5 RCPC encoded V-BLAST Architecture

A proper processing architecture is crucial to achieve high capacity potential [2] [7] [12]. V-BLAST is one of such architectures known to have spectral efficiencies of 20-40 bps/Hz at 24-34 dB average SNR without coding [7]. It is noted however that an appropriate coding scheme is required to complement the high data rate of the system with a high diversity gain.

In many wireless communication systems, convolutional codes are mostly used because of their capability to enable soft-decision decoding and their near Shannon-capacity performance [20]. However, with each additional bit in the encoder output, the complexity in their decoding process tends to increase and this may lead to erroneous decoding. One way to mitigate this problem is by using punctured convolutional codes, where several bits in the codewords produced by the encoders are deleted (punctured). One coding approach in which diversity gain and multiplexing gain are taken into consideration is the unequal error protection (UEP). The basic idea of this approach is to assign different levels of error protection to different data streams. By providing different levels of error protection, a high data redundancy is mitigated. This will in turn contribute to bandwidth efficiency. UEP can be attained using rate-compatible punctured convolutional (RCPC) codes, in which a single encoder and decoder structure is employed to provide different code rates, hence giving different levels of protection to the information source [3]. Several researches have proposed the use of UEP with MIMO scheme [13] [24]. The UEP proposed in these researches imply the need to resend information repeatedly using progressively stronger code protections, and therefore are more suitable for systems requiring automatic repeat request (ARQ). For wireless system communications where ARQ is typically not implemented, there is a need for a different way to have UEP.

In a coded system with unequal error protection (UEP), one way to achieve UEP is to arrange the binary information bits in groups according to their protection level and several channel encoders and decoders are employed, in parallel, to give the necessary error protections. The complexity of this system becomes impractical when the numbers of error sensitivity levels become large. Thus, a single channel encoder and decoder structure using rate-compatible punctured convolutional codes are suitable for this application.

3.5.1 Rate Compatible Punctured Convolutional (RCPC) Codes

3.5.1.1 Background and general properties

Punctured convolutional codes were first introduced by Cain, Clark, and Geist [38] mainly for the purpose of obtaining simpler Viterbi decoding for rate K/N codes with two branches arriving at each node instead of 2^K branches. They obtained codes of rate $2/3$ and $3/4$ by puncturing rate $1/2$ codes. These punctured codes were almost as good as the best known codes. Some of the good codes used the same basic rate $1/2$ generators. Later, Yasuda *et* al. [29, 32] found a family of $(N-1)/N$ codes by puncturing $1/2$ rate codes for N up to 14, and built selectable rate encoders and Viterbi decoders using soft decisions.

In [3] the concept of punctured convolutional codes is modified for the generation of a family of codes by adding a rate-compatibility restriction to the puncturing rule. The restriction implies that all the code bits of a high rate punctured code are used by the lower rate codes; or in other words, the high rate codes are embedded into the lower rate codes of the family. If the higher rate codes are not sufficiently powerful to decode channel errors, only supplemental bits which were previously punctured have to be transmitted in order to upgrade the code. Furthermore, since codes are compatible, rate variation within a data frame is possible to achieve unequal error protection.

Two important applications for RCPC codes are:

- Transmission channels with varying quality where the code rate is adapted by an automatic repeat request (ARQ) method (if a feedback channel is available) according to the channel properties. Typically, for a good channel only the punctured code is used and only if the channel quality is deteriorating the punctured positions are transmitted as well to raise the correctability [4].
- Data sources where the different bits within a frame have varying importance and therefore require a varying error protection. This is also called *unequal error protection (UEP) coding*. An interesting application is the source encoding of speech in digital mobile radio systems [47].

In general, a rate of $P/(P+l)$ rate compatible punctured convolutional code can be obtained by periodically puncturing a low-rate $R = 1/N$ code, memory M convolutional code having the generator tap matrix G with period P and $1 < l < (N-1)P$.

$$G = \left[\overbrace{\left(g_{ij} \right)}^{M+1} \right] \qquad (3.28)$$

The low-rate $R = 1/N$ code is called the mother code. The basic procedure for constructing a high-rate $R = P/(P+l)$ rate compatible punctured convolutional code from a rate-$R = 1/N$ code for $l = 1, 2, \ldots, (N-1)P$ can be described as encoding by the mother code followed by a puncturing device. The puncturing device deletes the encoded output symbols using an $N \times P$ puncturing matrix $a(l)$ with binary elements and $1 < l < (N-1)P$. Clearly, the rate of the punctured code is determined by the values of P and l.

$$a(l) = \left[\overbrace{\left(a_{ij}(l) \right)}^{P} \right] \qquad (3.29)$$

In order to explain what rate-compatible puncturing means, we use the simple example of Figure 3.11 where a rate $R = ½$ convolutional code with memory $M = 2$ is punctured periodically with period $P = 4$. We describe the binary information symbols and the binary *(0, 1)* code symbols by values ±1 where +1 corresponds to 0 and -1 corresponds to 1. A zero in the puncturing table *a(l)* means that the code symbol is not to be transmitted.

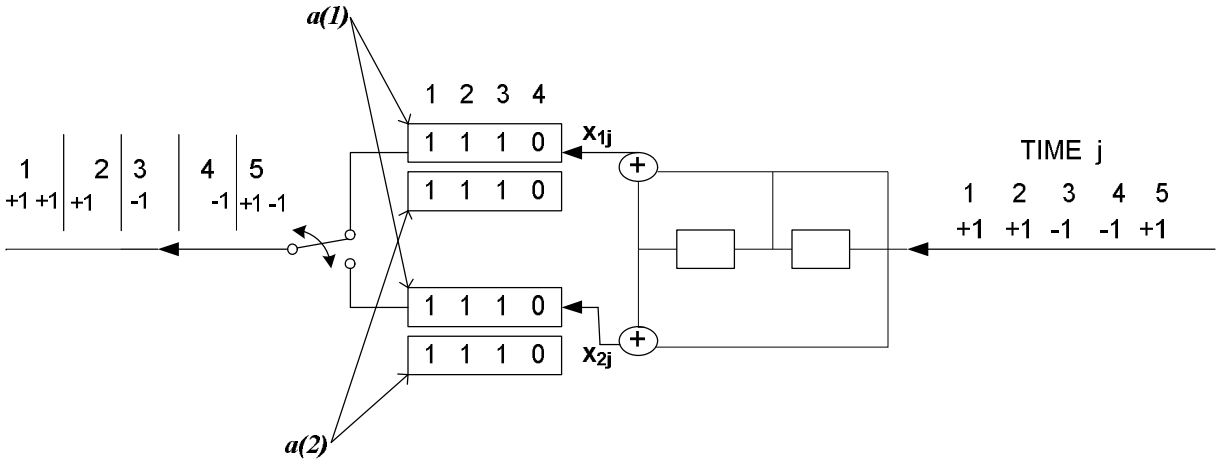

Figure 3.12: Example of two RCPC codes with N = 2, M = 2, P = 4 and two puncturing tables $a(1)$ and $a(2)$ with rates 4/5 and 4/6.

The index *l* defines the level of puncturing. In the above example of Figure 3.12 denoted by the label $a(1)$, the fourth bit of the upper branch, the second and third bits of the lower branch are not transmitted. The puncturing table can be viewed as a modulo *P* rule for multiplexing the two streams of code bits. Instead of transmitting 2P = 8 bits, only $P + l = 5$ bits are transmitted per $P = 4$ information bits. Therefore, we have generated a rate 4/5 code which is embedded into the rate 1/2 mother code. The lower table in the example results in a code of rate 4/6 = 2/3**.** The code in the example is completely described by the tap matrix G of the shift register

$$G = \begin{pmatrix} 1 & 1 & 1 \\ 1 & 0 & 1 \end{pmatrix} \qquad (3.30)$$

and the puncturing matrices

$$a(1) = \begin{pmatrix} 1 & 1 & 1 & 0 \\ 1 & 0 & 0 & 1 \end{pmatrix} \qquad (3.31a)$$

$$a(2) = \begin{pmatrix} 1 & 1 & 1 & 0 \\ 1 & 1 & 0 & 1 \end{pmatrix} \qquad (3.31b)$$

The general puncturing matrix *a(l)* for a mother code of rate l/N and a puncturing period of *P* has *N* rows and *P* columns**.** The parameter *l* describes the order of the puncturing. The number

of zeros in the puncturing table is *(N - l)P -1***.** As we go to a lower rate code in the above example, we allow new "1's" in the puncturing matrix only in previously punctured positions and retain the previous "1's." This means that all the bits of the high rate code are used by the low rate code. If $a_{ij}(l_o)$ = 1, then

$$a_{ij} = 1 \text{ for all } l \geq l_o \geq 1. \qquad (3.32)$$

Equation (3.32) is called the *rate compatibility restriction.*

To obtain a rate 4/7 code, we have only two choices in arriving at *a(3)* using (3.31). Generally, from a mother code of rate 1/*N*, we obtain a family of codes with rates

$$R = \frac{P}{P+l} \qquad l = 1, 2, \ldots, (N-1)P \qquad (3.33)$$

All high rate codes are embedded into the lower rate codes.

3.5.1.2 system model

A block diagram of the end-to-end communication system for unequal error protected data transmission using RCPC codes is shown in Figure 3.13. For a slow frequency nonselective fading channel, the received signal can be represented by an equivalent low-pass signal sampled at time *m* :

$$y[m] = a_f[m]x[m]+n[m] \qquad (3.34)$$

where *x[m]* is the transmitted signal, *n[m]* is a sample of a zero-mean complex Gaussian noise process with variance σ^2 and $a_f[m]$ is the amplitude of the channel gain.

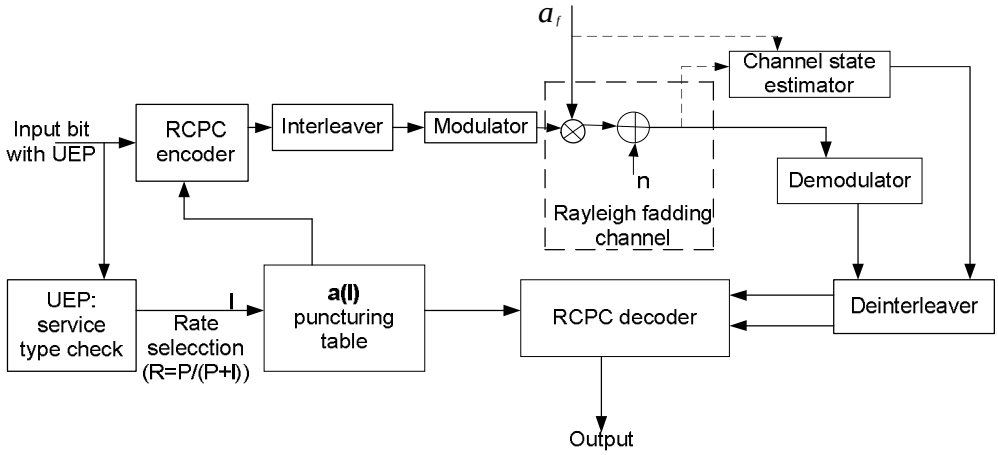

Figure 3.13: unequal error protected data transmission using RCPC codes on Rayleigh fadding channel

The channel has time-varying amplitude fading $a_f[m]$, AWGN *n[m],* and no intersymbol interference is assumed. In our numerical results we assume the amplitude variations follow a Rayleigh distribution. The interleaver/deinterleaver pair are assumed to have infinite depth so that the amplitude values appear i.i.d. to the channel decoder.The encoder uses the same shift register for all code rates. Only the multiplexer rule is changed, and the multiplexer will function according to the puncturing rule *a(l).* The parameter *l* can be changed during the transmission as long as the decoder uses the same sequence of puncturing rules for proper demultiplexing.

On the receiver side, the Viterbi algorithm is used for decoding. The VA utilizes the sequences of received signals and the channel state information to perform the maximum likelihood (ML) decision on a possible sequence of transmitted signals. With RCPC codes, the VA is performed exactly as with standard convolutional codes, except that the decoder must know the puncturing matrix currently in use and should not update branch metrics at positions occupied by deleted digits. The basic description of Viterbi algorithm has been presented in [21].

3.5.1.3 Error-Probability Analysis of RCPC Codes

The performance of punctured convolutional codes are determined by the following parameters [21] [4].

a) The minimum free distance of the code, d_{free}

b) The number of incorrect paths whose distance $d \geq d_{free}$, diverging from the correct path to re-emerge with it at a later stage, a_d

c) The number of erroneous bits produced by the incorrect paths, c_d

d) The probability that an incorrect path is picked out during the Viterbi decoding process, P_d

It has been shown [3] that for $N \leq 4$, $P \leq$ **8,** and $M \leq 6$, code families with non-catastrophic codes exist, which are almost as good as the best known high rate convolutional codes. Based on this we choose a typical RCPC code which is shown in table 2, where rate compatible punctured codes with rates from 8/9 to 1/4 are derived from a rate 1/4 mother code with the generator matrix

$$G(x) = (1+x^3 + x^4,\ 1 + x + x^2 + x^4,\ 1 + x^2 + x^3 + x^4,\ 1 + x + x^3 + x^4) \qquad (3.35)$$

Table 2**:** Puncturing tables *a(l)*,c_d, d_f, and a_d values for RCPC codes with memory *M=4*, period *P=8* , *N=4* and rates *R=P/(P+l)=8/(8+l)*, *l*= 1, 2, 4, 6, ..., 24

RCPC Codes (M=4 P=8) **Generator Matrix**

$$G = \begin{pmatrix} 10011 \\ 11101 \\ 10111 \\ 11011 \end{pmatrix}$$

Rate	8/9	8/10	8/12	8/14	8/16	8/18	8/20	8/22	8/24	8/26	8/28	8/30	8/32
a(l)	*1111 0111 1000 1000 0000 0000*	*1111 1111 1000 1000 0000 0000*	*1111 1111 1010 1010 0000 0000*	*1111 1111 1110 1110 0000 0000*	*1111 1111 1111 1111 0000 0000*	*1111 1111 1111 1111 1000 1000*	*1111 1111 1111 1111 1100 1100*	*1111 1111 1111 1111 1110 1110*	*1111 1111 1111 1111 1111 1111*	*1111 1111 1111 1111 1111 1111 1000 1000*	*1111 1111 1111 1111 1111 1111 1010 1010*	*1111 1111 1111 1111 1111 1111 1110 1110*	*1111 1111 1111 1111 1111 1111 1111 1111*
$\mathbf{d_f}$	2	3	4	5	6	7	8	9	10	11	12	13	14
$\mathbf{c_d}$	1	42	4	2	0	2	2	10	0	2	0	2	0
		242	274	0	62	32	36	34	8	8	4	20	16
			4199	2688	496	144	96	60	28	36	48	56	20
$\mathbf{a_d}$	1	8	4	2	0	2	2	4	0	2	0	2	0
		30	40	0	18	16	14	14	6	8	4	12	8
			327	274	108	32	24	18	10	14	16	20	12

We will use it for our simulations in order to analyze performance bound trends of RCPC codes and code rate allocation to support a target BER for a given signal to noise ratio.

A zero in the puncturing pattern indicates puncturing. In table 2 the first group of 8 bits in the puncturing matrix *a(l)* refers to first generator polynomial, the second group to the second polynomial, and so on.

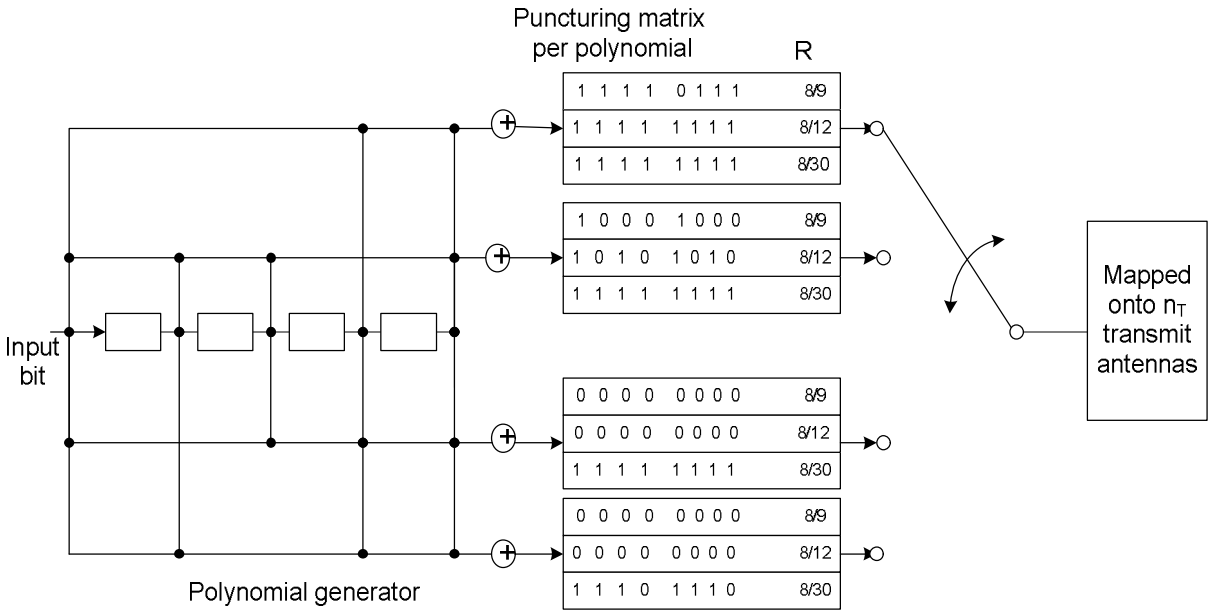

Figure 3.14: RCPC encoder with three exemplary code rates (mother code rate with M=4 and P=8)

The RCPC encoder for three exemplary code rates is shown in detail in Figure 3.14, although all necessary information is already contained in table 2. For code rates greater than or equal to 1⁄2 only the two first polynomials from $\boldsymbol{G}(x)$ are used.

From [11], we have seen that by analyzing the speech coder, information about the relative importance or susceptibility to errors in the bits representing the speech can be obtained. We call this type of information the source significance information (SSI) or error sensitivity information. An example of SSI would be the required bit error rate (BER) after channel decoding for single bits or for a certain group of bits. Assume that we have a block of $\boldsymbol{n}$ information bits divided into K groups, with the $\boldsymbol{n_k}$ information bits in the k^{th} group requiring a BER of P_k after decoding. In this case, P_k would be the SSI and

$$\sum_{k=1}^{K} \boldsymbol{n_k} = \boldsymbol{n} \qquad (3.36)$$

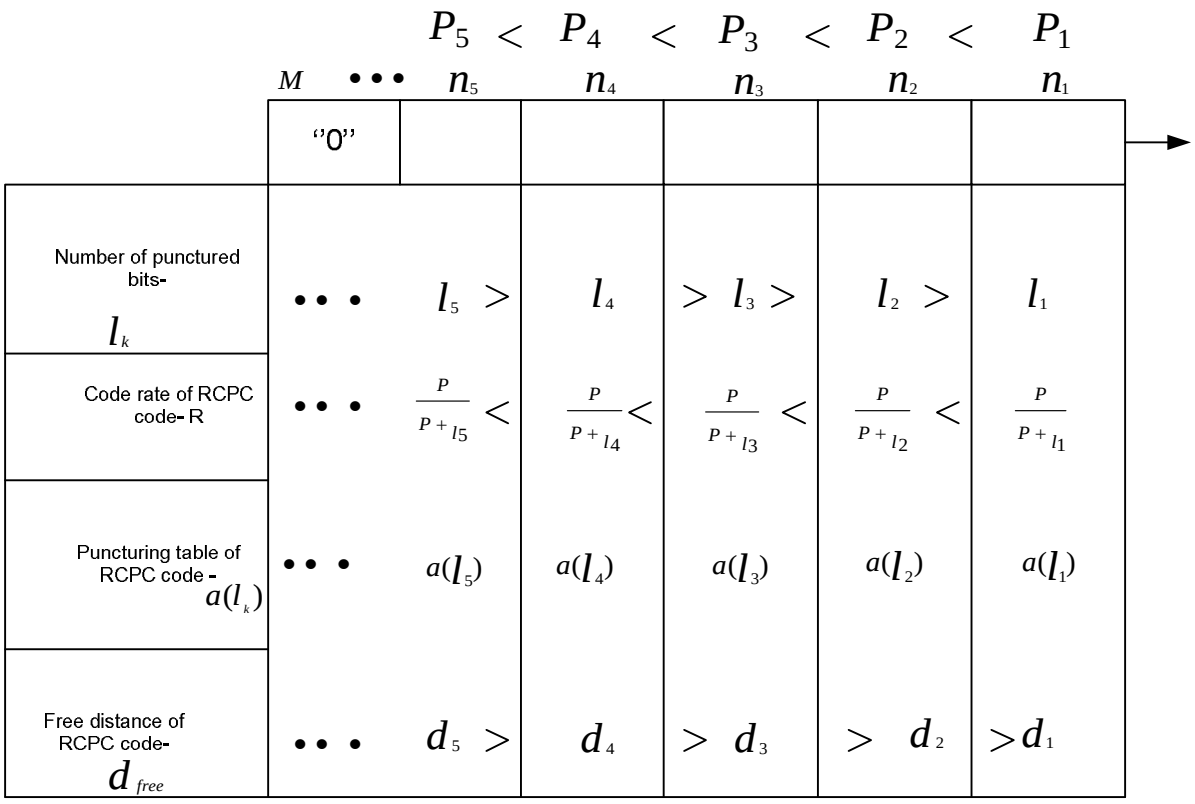

Figure 3.15: Assignments of RCPC codes to an information block with bits grouped according to their error sensitivity.

An example is given in Figure 3.15 where we have ordered the information bits according to their relative importance and their corresponding error protection need P_k **.** Where n_1, n_2, n_3, ... are the block length of the RCPC codes with the corresponding error protection level of P_1 , P_2 , P_3, ... respectively. A group of *M* known bits, e.g., zeros, is added for proper termination of the decoding process. M is the memory of the convolutional encoder. Of course, one could now separately encode the K groups by K different encoders and use K different decoders according to the protection needs. Besides the increased overhead and complexity, the upper bound on the overall delay will imply that for some groups, $\boldsymbol{n_k}$ might be rather small, resulting in the exclusion of powerful long channel codes. Here, we wish to use *one* encoder and *one* decoder, which provides the protection requirements within one data frame with a minimum of redundancy and overhead. This can be achieved by modifying the concept of punctured

convolutional codes in [29] & [38] by introducing a rate compatibility restriction to the puncturing rule [3].

In applying unequal error protection to the bits in a data frame, the bits should be ordered according to their significance, starting with the bits which require the least protection. This has been shown in Figure 3.15. During the $\boldsymbol{n_1}$ information bits, the puncturing matrix $a(l_1)$ is used as the relevant rule for the multiplexer. As soon as the first bit of the second group enters the encoder, the puncturing table $a(l_2)$ will be used. After another $\boldsymbol{n_2}$ information bits or encoder shifts, the table is switched to $a(l_3)$, etc. At the k^{th} step, $P + l_k$ code bits are transmitted per P information bits using the RCPC code with index l_k, puncturing table $a(l_k)$, free distance d_k, and rate $P / (P + l_k)$. The frame is terminated after group K by shifting M *"0"* bits into the shift register, thus transmitting $M(P + l_k)/P$ overhead code bits necessary for proper termination of the trellis in the all-zero state. The average effective code rate is then

$$R_{av} = \frac{\sum_{k=1}^{K} \boldsymbol{n_k} P}{\left(\sum_{k=1}^{K} \boldsymbol{n_k}(P+l_k)\right)+M(P+l_k)} \tag{3.37}$$

The rate compatibility condition given in **(**3.32) is very important. In a transitional phase between two matrices $a(l_1)$ and $a(l_2)$ where $l_2 > l_1$, we have to be sure that despite the transition, the distance properties of all paths originating in code l_1 do not suffer a loss of distance due to transitions, thus guaranteeing at least the designed performance.

For any rate-K/N codes with Viterbi decoding on discrete memoryless channels, the upper bound on the error event and bit error probabilities [17] are given by

$$P_e \leq \frac{1}{P}\left(\sum_{d=d_{free}}^{\infty} a_d \, P_d\right) \tag{3.38}$$

and

$$P_b \leq \frac{1}{P}\left(\sum_{d=d_{free}}^{\infty} c_d \, P_d\right) \tag{3.39}$$

respectively. Here, d_{free} is the minimum free distance of the code, a_d is the number of incorrect paths of Hamming weight d for $d \geq d_{free}$ that diverge from the correct path and re-emerge with it

at some later stage, c_d is the total number of error bits produced by the incorrect paths, and P_d is the probability of picking an incorrect path in the Viterbi decoding process and depends on the modulation type and channel characteristics.

For a Rayleigh fading channel with soft decision on y and full CSI, P_d is upper bounded [46] by

$$P_d \leq \frac{1}{2}\left(\frac{1}{1+\gamma R}\right)^d \qquad (3.40)$$

3.5.2 RCPC encoded V-BLAST System model

The system model for RCPC encoded V-BLAST scheme is depicted in Figure 3.16. The channel is assumed to undergo Rayleigh fading and there exists a rich scattering paths between the transmit and receive antennas. on the transmitter side, the input bit stream is partitioned according to the relative importance of each bits. The highest error protection level, which is given by the lowest code rate, is assigned to the bits of highest importance [3, 4, 24, 31]. These code rates are assigned by RCPC encoder for which a puncturing table *a(l)* is fed as a reference.

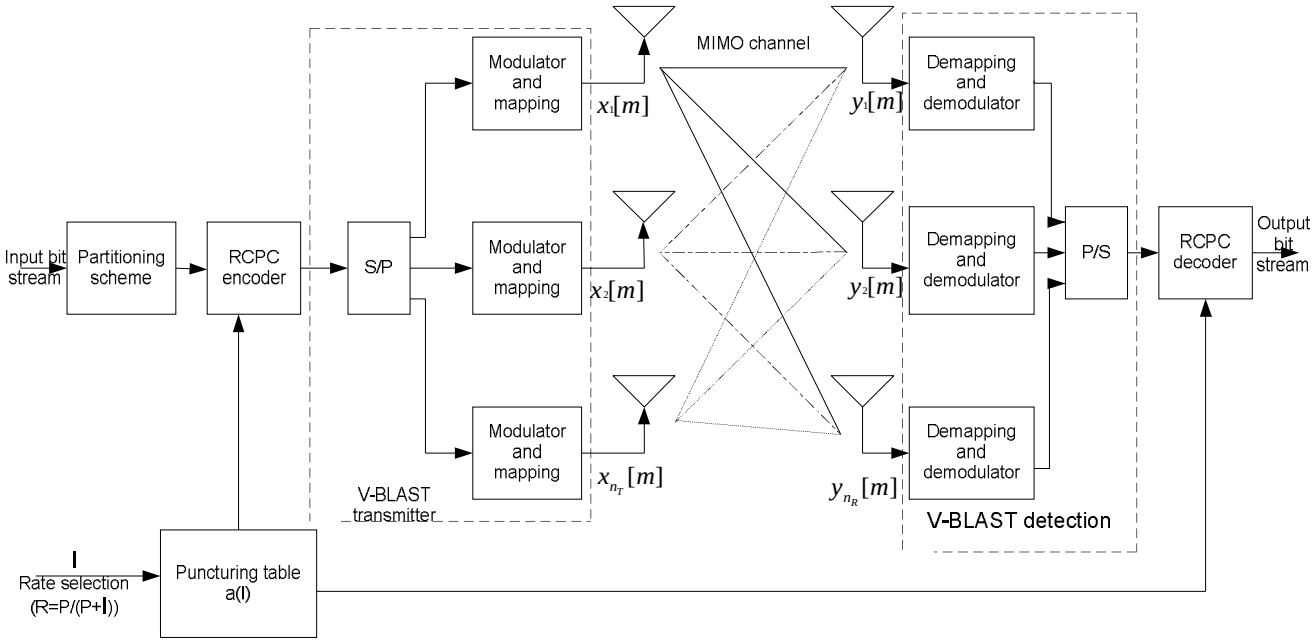

Figure 3.16: system model for RCPC encoded V-BLAST MIMO

The elements of a signal vector $x[m]$: $x_1[m], x_2[m], \ldots, x_{n_T}[m]$ are transmitted simultaneously from first to the m^{th} transmit antennas, and the signal vector arriving at the receive antennas $\mathbf{y}[m]$: $y_1[m], y_2[m], \ldots, y_{n_T}[m]$ can be expressed as

$$y[m] = Hx[m] + n[m] \tag{3.41}$$

where H is the matrix channel of a MIMO system whose elements are the channel gains between the transmit and receive antennas, $y[m]$ is the received symbol vector, $x[m]$ is the transmitted symbol vector and $n[m]$ is a noise vector with complex Gaussian distribution, zero mean and variance σ^2.

For instance the received signal at antenna n_R can be expressed as

$$y_{n_R}[m] = \left(h_{n_{R1}} x_1[m] + n_1[m]\right) + \left(h_{n_{R2}} x_2[m] + n_2[m]\right) + \cdots + \left(h_{n_R n_T} x_{n_T}[m] + n_{n_R}[m]\right) \quad (3.42)$$

The performance measure of RCPC encoded V-BLAST system is the probability that the signal estimated at the receiver does not match the transmitted signal. This is a function of the system modulation, fading channel coefficients, and the performance of error correction codes used. The bit error probability of RCPC codes follows that of a Viterbi criterion [17]

$$P_{b\ RCPC} \leq \frac{1}{P}\left(\sum_{d=d_{free}}^{\infty} c_d\, P_d\right) \tag{3.43}$$

Where P is the puncturing period, d_{free} is the minimum free distance of the code, c_d is the total error bits produced by the incorrect paths and P_d is the probability of picking the incorrect path in Viterbi decoding process and is influenced by the modulation type. In this thesis, both d_{free} and c_d used are taken from [3] and are given in table 2.

Rectangular QAM signal constellation have the distinct advantage of being easily generated as two PAM signals impressed on phase-quadrature carriers. In addition, they are easily demodulated. Although they are not the best M-ary QAM signal constellation for $M \geq 16$, the average transmitted power required to achieve a given minimun distance is only slightly greater than the average power required for the best M-ary QAM signal constellation [16]. For these reasons, the modulation used for this part is rectangular M-QAM where M denotes the

constellation size of the signal, M = 2^k points (k even). For QAM with even number of bits per symbol, the probability of symbol-error per carrier is [16, 31]

$$P_{SC} = 2\left(1 - \frac{1}{\sqrt{M}}\right) Q\left(\sqrt{\frac{3E_S}{(M-1)N_O}}\right) \quad (3.44)$$

Where *Es* is the energy per symbol, *No* denotes the noise power spectral density, and *Q(α)* is a normalized form of the cumulative normal distribution function. The modulators and demodulators use rectangular QAM constellation. The probability of symbol-error is therefore approximated by [16]

$$P_S = 1 - (1 - P_{SC})^2 \quad (3.45)$$

The bits are assigned to symbols using Gray-coded assignment with equal number of bits per carrier, hence the probability of bit-error per carrier is approximated by [16, 31]

$$P_{bc} = \frac{4}{k}\left(1 - \frac{1}{\sqrt{M}}\right) Q\left(\sqrt{\frac{3kE_b}{(M-1)N_O}}\right) \quad (3.46)$$

The probability of bit-error for rectangular QAM is consequently approximated by [6, 16, 31].

$$P_b = 1 - (1 - P_{bc})^2 \quad (3.47)$$

Therefore, including the bit-error probability of the modulation used, the fading channel characteristics and the bit-error probability of RCPC codes yields the equation for RCPC-encoded V-BLAST MIMO system:

$$P_{bRCPC\ encoded\ V-BLAST} = \frac{1}{P}\left(\sum_{d=d_{free}}^{\infty} c_d \left(1 - \left(1 - \frac{4}{k}\left(1 - \frac{1}{\sqrt{M}}\right)\left(\frac{1}{2} - \frac{1}{2} erf\left(\sqrt{\frac{3.k.\gamma.R}{2(M-1)}}\right)\right)\right)\right)\right) \quad (3.48)$$

Where *k* is the number of bits per symbol and γ denotes the average signal-to-noise ratio at the Rx antennas of a MIMO system.

Chapter 4

Simulation results and discussion

This Chapter presents the simulation results of the general V-BLAST architecture with different detectors in Matlab software. We will also discuss performance and complexity trade-off comparision of these detectors, performance bound trends of RCPC codes with the mother code rate of ¼ and UEP analysis of RCPC encoded V-BLAST system.

4.1 System model

In this simulation, the fading channel characteristics are assumed to be known perfectly at the receiver. The transmitter consists of a binary random generator, a binary phase shift key (BPSK) baseband modulator and a vector encoder. The binary random generator generates the transmitted bits. These bits are modulated in the BPSK modulator. The vector encoder maps the symbols to each antenna.

In the channel block, the transmitted symbols undergo Rayleigh fading and additive noise. In addition, the channel is assumed to be quasi-stationary, and that is, the channel coefficients do not vary during the signal duration.

The receiver is made up of decoding processing and an error rate calculation block. The decision device approximates the decoder output to one of the possible symbols from the symbol set. A comparison is made between the transmitted and received symbols to obtain number of errors. This number, when divided by the total number of transmitted symbols, yields the BER for the system.

At the decoding processing block, we will simulate the $2 \times n_R$ general V-BLAST architecture and investigate the performance with ML, ZF, MMSE, the SIC and the OSIC detectors.The optimum ML is taken as a bench mark and also the 1x1 antenna arrangement theoretical simulation output is also included for comparision.

The Antenna arrangement $2 \times n_R$ is chosen because in 3GPP it has been stated that advanced MIMO techniques could employ up to 4 receive antennas, while keeping the transmitted layers to be 2 [48].

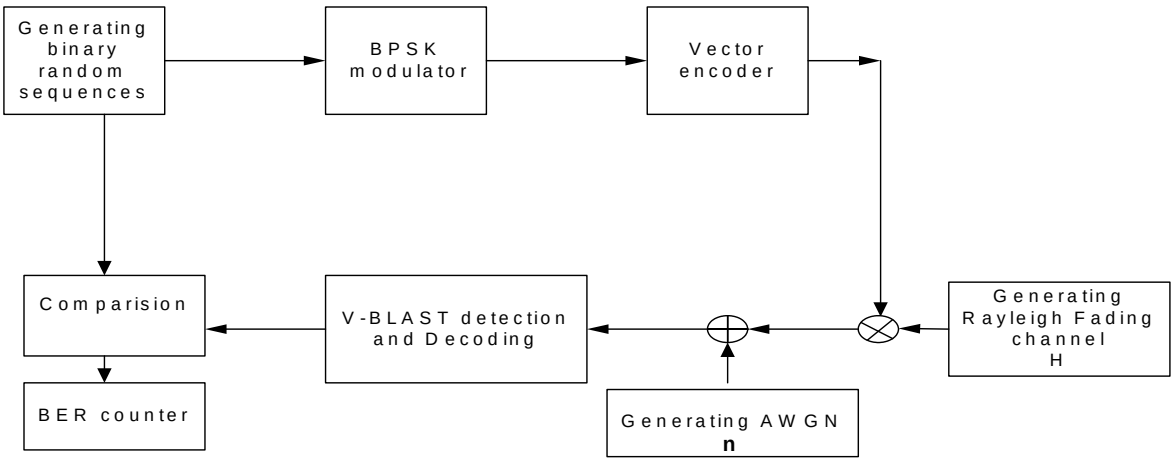

Figure 4.1 Simulation system model

4.2 Simulation parameters and outputs

Tabe 3: Simulation parameters

System	V-BLAST
# transmit antenna	2
# receieve antenna	n_R
channel	Rayleigh flat fading, quasi-static
Noise	AWGN
Modulation	BPSK
Detectors	ML, ZF and MMSE (together with SIC algorithm and ordering)
No. of transmission bits or symbols	1.2*10^5
Channel state information	Perfectly known at the receiver
Channel coding	No coding
SNR range	0 to 20
# of iteration	100

We also use the following additional specification for RCPC codes in order to analysis performance bound trends of RCPC codes and UEP performance analysis of RCPC encoded V-BLAST MIMO System.

- Mother code with rate ¼
- The number of memory M=4
- The Puncturing period P=8
- The generator tap matrix G(x) = $(1+x^3 + x^4, 1 + x + x^2 + x^4, 1 + x^2 + x^3 + x^4, 1 + x + x^3 + x^4)$ = (10011, 11101, 10111, 11011)
- The distance spectra and the puncturing matrices are given in detail in Table 2

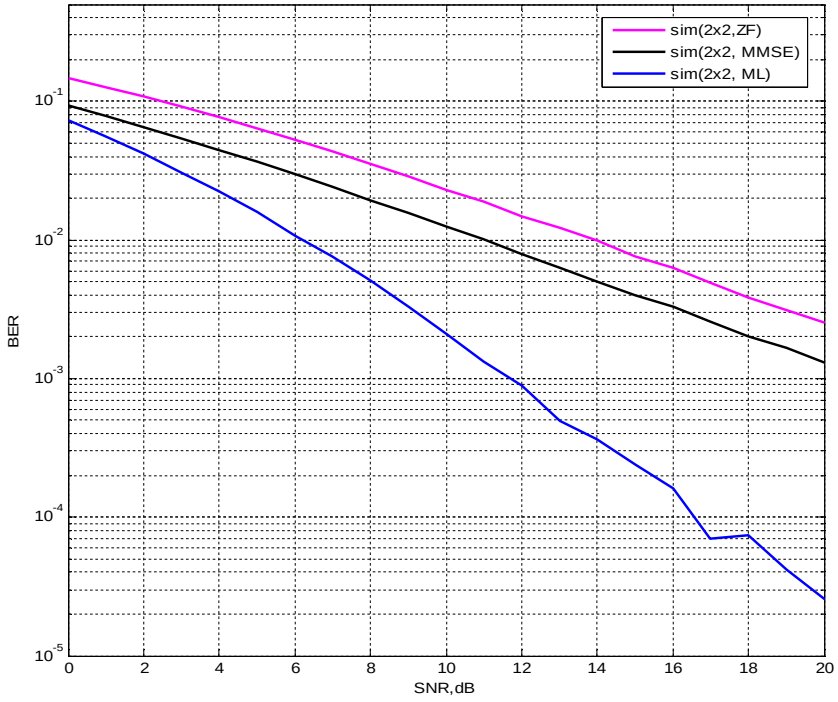

Figure 4.2: BER for BPSK modulation with 2x2 V-BLAST MIMO and ZF, MMSE & ML Detectors in Rayleigh fadding channel

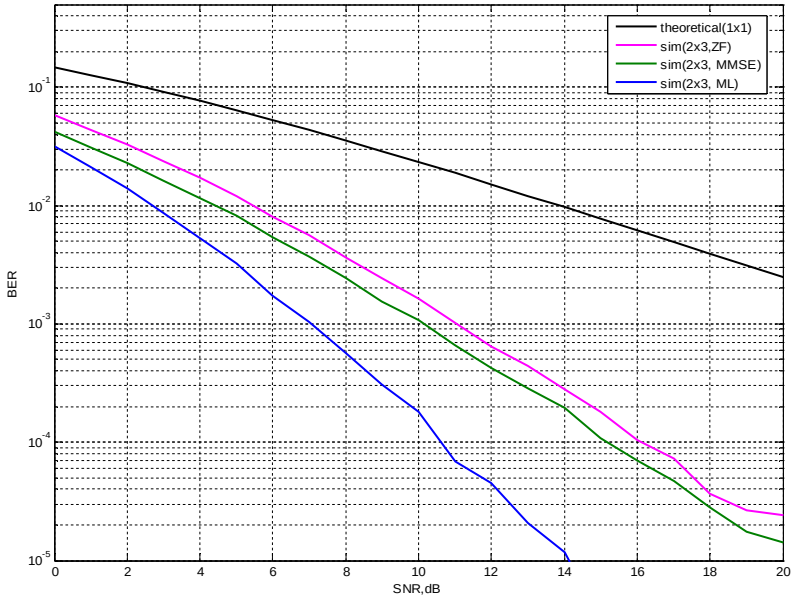

Figure 4.3: BER for BPSK modulation with 2x3 V-BLAST MIMO and ZF, MMSE & ML Detectors in Rayleigh fadding channel

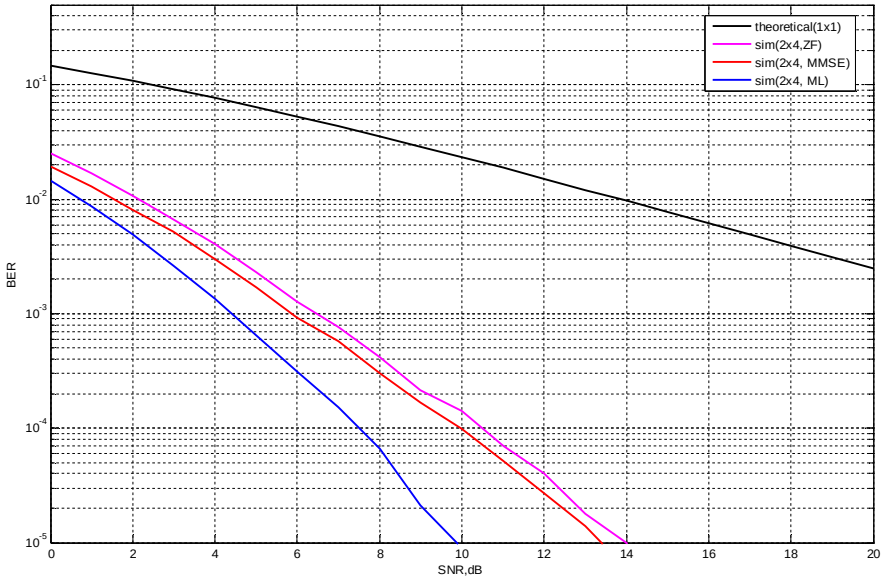

Figure 4.4: BER for BPSK modulation with 2x4 V-BLAST MIMO and ZF, MMSE & ML Detectors in Rayleigh fadding channel

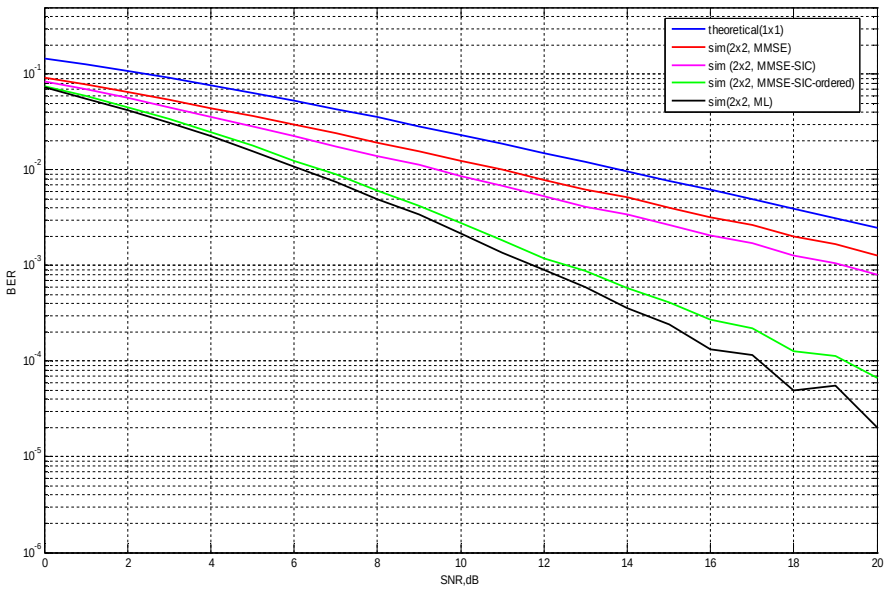

Figure 4.5: BER for BPSK modulation with 2x2 V-BLAST MIMO and MMSE, MMSE-SIC, MMSE-SIC-Ordered & ML Detectors in Rayleigh fadding channel

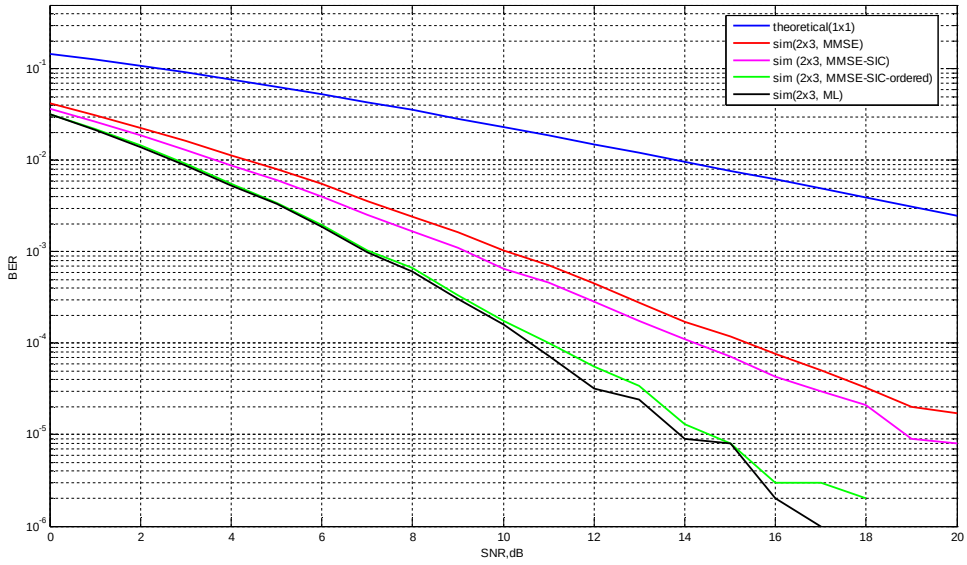

Figure 4.6: BER for BPSK modulation with 2x3 V-BLAST MIMO and MMSE, MMSE-SIC, MMSE-SIC-Ordered & ML Detectors in Rayleigh fadding channel

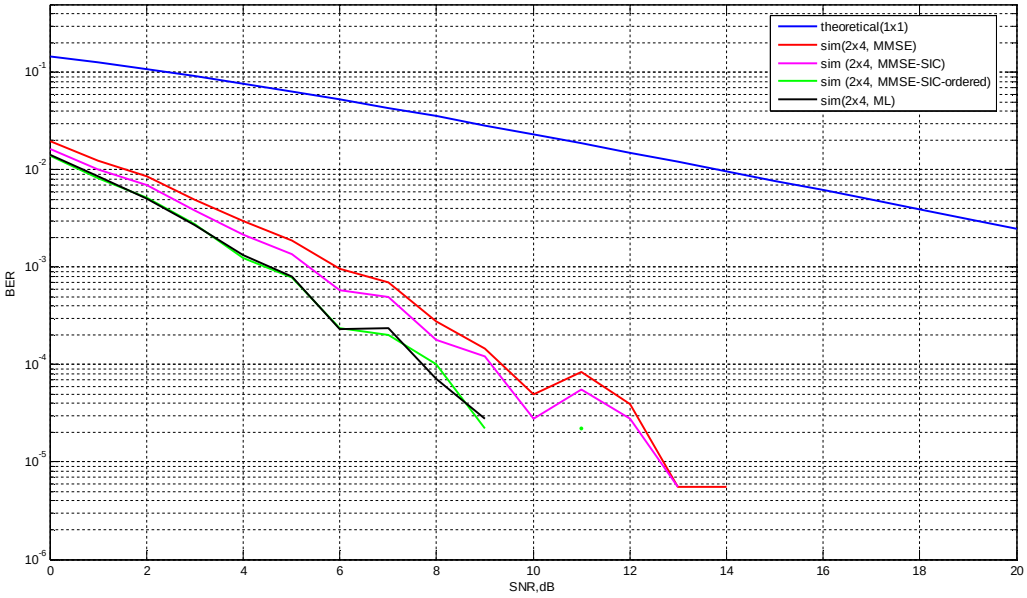

Figure 4.7: BER for BPSK modulation with 2x4 V-BLAST MIMO and MMSE, MMSE-SIC, MMSE-SIC-Ordered & ML Detectors in Rayleigh fadding channel

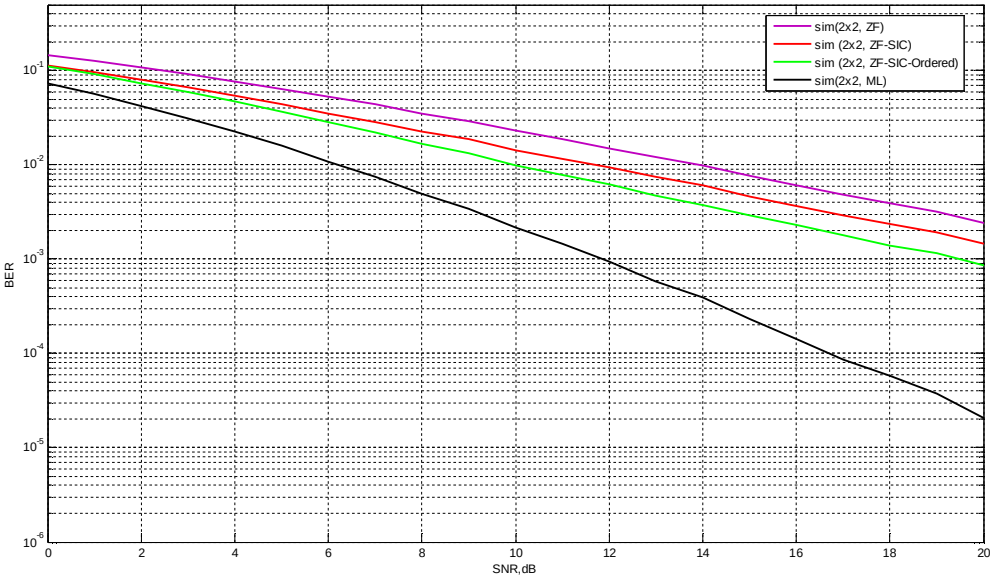

Figure 4.8: BER for BPSK modulation with 2x2 V-BLAST MIMO and ZF, ZF-SIC, ZF-SIC-Ordered & ML Detectors in Rayleigh fadding channel

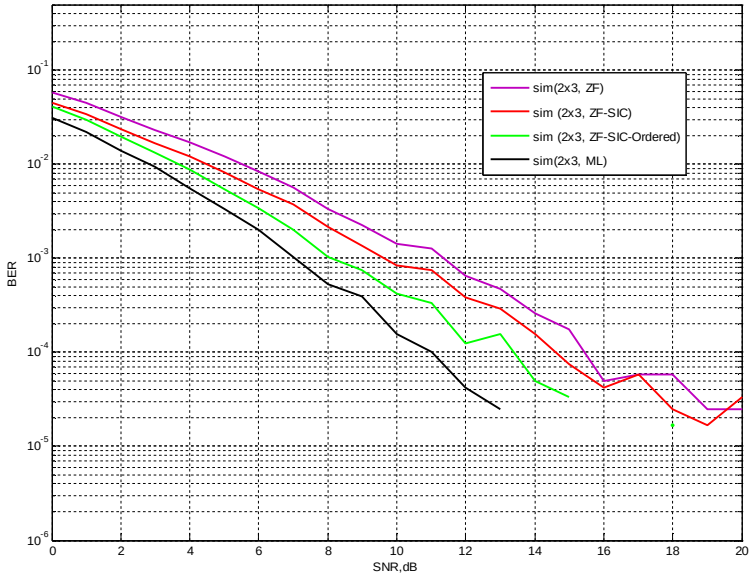

Figure 4.9: BER for BPSK modulation with 2x3 V-BLAST MIMO and ZF, ZF-SIC, ZF-SIC-Ordered & ML Detectors in Rayleigh fadding channel

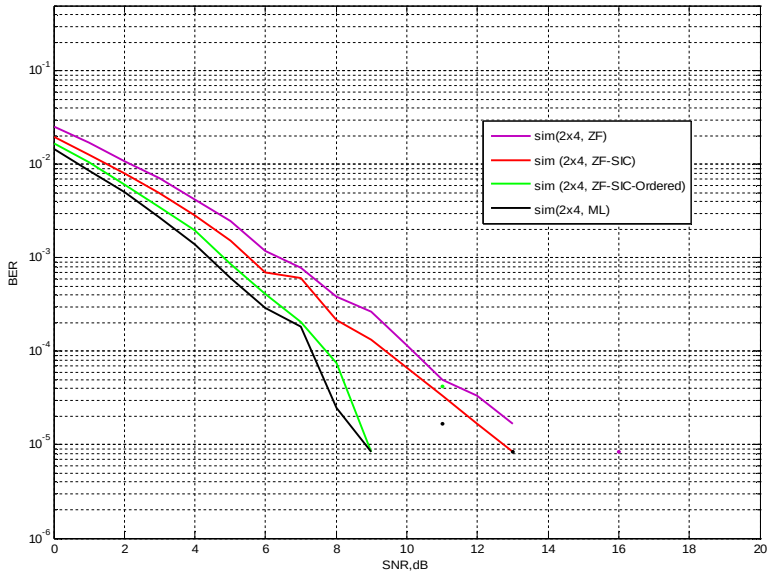

Figure 4.10: BER for BPSK modulation with 2x4 V-BLAST MIMO and ZF, ZF-SIC, ZF-SIC-Ordered & ML Detectors in Rayleigh fadding channel

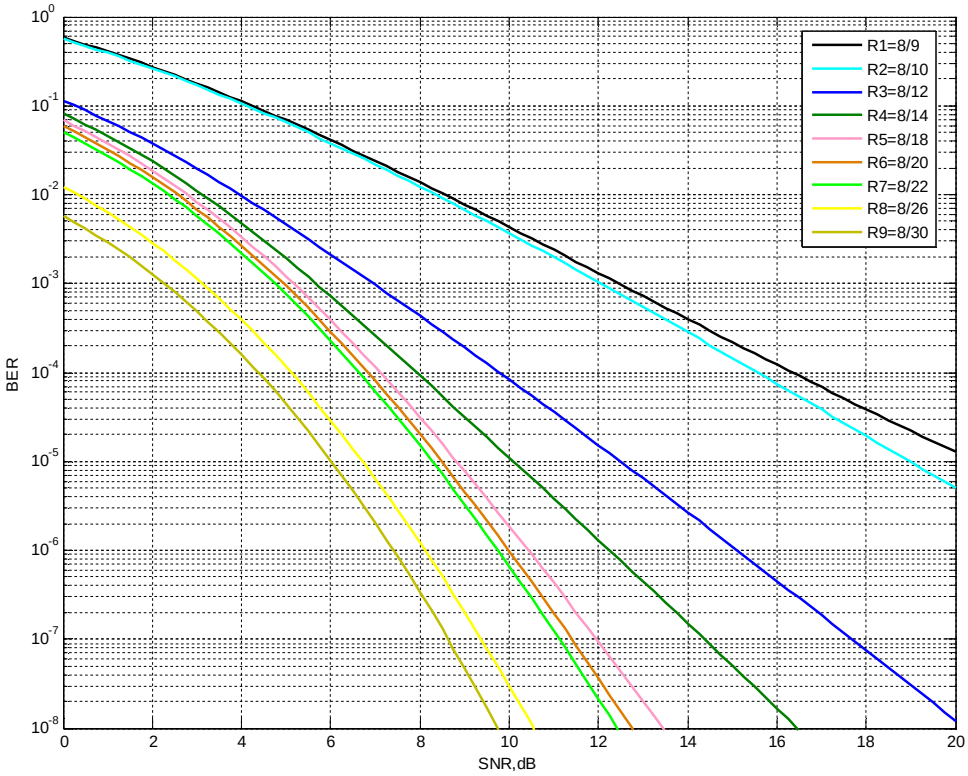

Figure 4.11: BER performance of RCPC codes on Rayleigh fading channel (P=8, N=4)

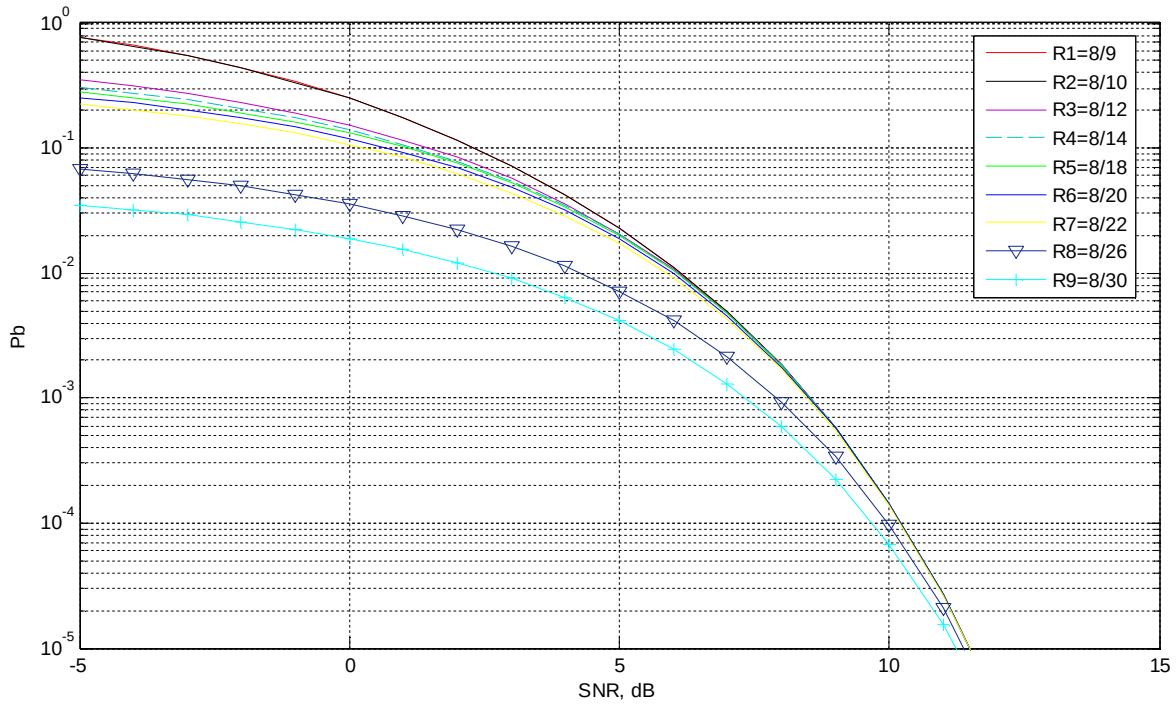

Figure 4.12: BER performance of RCPC encoded V-BLAST MIMO system with (N = 4 & P = 8)

3.3 Discussions

For our simulation results, we calculate the performances based on the average of 100 different channel realizations for each (n_T, n_R) MIMO system. In order to have nearly smooth simulations outputs, the number of realizations and transmission bits are chosen to be large enough.

A. Performance of V-BLAST MIMO Systems in Rayleigh-fading Channels with *ZF, MMSE & ML Detectors.*

Figure 4.2 to 4.4 shows all the simulation results with ZF, MMSE & ML Detectors. The sample data values for all these detectors at a certain constant SNR (e.g 8dB) to show the performance improvment (BER) and at a certain constant BER (0.01) to show the power margin improvment for the 2x2, 2x3 and 2x4 antenna arrangements is shown in Table 4 below.

For 2x2 V-BLAST system, at BER of 0.01, there is approximately 3 dB SNR difference between the MMSE and ZF detectors. The ML Detector detector shows 8 dB improvements than the ZF one. The ML detector shows highest power margin improvement among these detectors.

For 2x2 V-BLAST system, at SNR of 8dB, there is approximately a BER of 3.45*1o^-2 with ZF, 1.8*10^-2 with MMSE, 4.8*10^-3 with ML detector. These shows that there is performance improvement of MMSE and ML detectors than the ZF detector. This logic applies for the rest of antenna arrangements and their values are given in Table 4. But this performace improvement for ML detector is brought at the expense of increasing system complexity as shown in Figures 3.10 & 3.11. From Figure 3.11, the computational complexity of the ZF, MMSE and ML detectors are respectively on the order of 9x10^2, 9x10^2 and 5.8x10^4 for BPSK modulation and 2x2 V-BLAST system. The ML detector is around 65 times computational complex than ZF and MMSE for this antenna arrangement and modulation used.

Table 4: Sample data (at constant SNR=8 & constant BER=10^-2) for ZF, MMSE & ML detectors

Antenna arrangement	BER at 8dB SNR			SNR in dB at BER of 10^-2		
	ZF	MMSE	ML	ZF	MMSE	ML
2X2	3.45*1o^-2	1.8*10^-2	4.8*10^-3	14	11	6.00
2X3	3.56*10^-3	2.36*10^-3	5.4*10^-4	5.56	4.5	2.74
2X4	4.00*10^-4	3*10^-4	6.5*10^-5	2.22	1.5	.90

B. Performance of V-BLAST MIMO Systems in Rayleigh-fading Channels with MMSE, MMSE-SIC, MMSE-SIC-Ordered & ML Detectors

Figures 4.5 to 4.7 show all the simulation results with MMSE, MMSE-SIC, MMSE-SIC-Ordered & ML Detectors. The sample data values for all these detectors at a certain constant SNR (8dB) to show the performance improvment (BER) and at a certain constant BER (0.01) to show the power margin improvment for the 2x2, 2x3 and 2x4 antenna arrangements is shown in table 5 below.

For 2x2 V-BLAST system, at BER of 0.01, there is approximately 1.6 dB SNR difference between the MMSE-SIC and MMSE detectors. The MMSE-SIC-Ordered detector shows a 3.2 dB improvement than the MMSE one. The ML detector shows highest power margin improvement (3.8 dB). By using the SIC and OSIC, we approach the maximum likelihood detector power margin with less complexity cost (see Figures 3.10 & 3.11 for complexity comparision).

For 2x2 V-BLAST system, at SNR of 8dB, there is approximately a BER of 1.8*10^-2 with MMSE, 1.32*10^-2 MMSE-SIC, 5.85*10^-3 with MMSE-SIC-Ordered and 4.9*10^-3 with ML detector. These shows that there is continuous performance improvement by using the non-linear (SIC and OSIC) detectors with less complexity cost and this is true for the rest of antenna arrangements and their values are given in Table 5. The computational complexity of the MMSE, MMSE-OSIC and ML detectors are respectively on the order of 9x10^2, 2x10^3 and 5.8x10^4 for BPSK modulation and 2x2 V-BLAST system (Figure 3.10). The ML detector is around 29 times computational complex than MMSE-OSIC for this antenna arrangement and modulation used with almost similar BER performance (Figure 4.5). Also the average performance is improved when the number of receive antenna increases due to the extra receive diversity gain. When an extra receive antenna is added, the performance of different V-BLAST detection systems tends to be similar.

Table 5: Sample data(at constant SNR=8 & constant BER=10^-2) for MMSE, MMSE-SIC, MMSE-SIC-Ordered & ML detectors

Antenna arrangement	BER at 8dB SNR				SNR in dB at BER of 10^-2			
	MMSE	MMSE-SIC	MMSE-SIC-Ordered	ML	MMSE	MMSE-SIC	MMSE-SIC-Ordered	ML
2X2	1.8*10^-2	1.32*10^-2	5.85*10^-3	4.9*10^-3	11	9.4	6.8	6.2
2X3	2.4*10^-3	1.67*10^-3	6.67*10^-4	6.02*10^-4	4.3	3.8	2.9	2.8
2X4	3*10^-4	1.78*10^-4	10^-4	7.2*10^-5	1.5	1	.8	.9

C. Performance of V-BLAST MIMO Systems in Rayleigh-fading Channels with ZF, ZF – SIC, ZF-SIC Ordered & ML Detectors.

Figures 4.8 to 4.10 show all the simulation results with ZF, ZF–SIC, ZF-SIC Ordered & ML Detectors. The sample data values for all these detectors at a certain constant SNR (8dB) to show the performance improvment (BER) and at a certain constant BER (0.01) to show the power margin improvment for the 2x2, 2x3 and 2x4 antenna arrangements is shown in Table 6 below.

For 2x2 V-BLAST system, at BER of 0.01, there is approximately 3.5 dB SNR difference between the ZF–SIC and ZF detectors. The ZF–SIC ordering detector shows a 4.2 dB improvement than the ZF one. The ML detector shows highest power margin improvement among these detectors (7.8 dB). By using the SIC and OSIC, we can approach the maximum likelihood detector power margin with less complexity cost.

For 2x2 V-BLAST system, at SNR of 8dB, there is approximately a BER of 3.4*10^-2 with ZF, 2.2*10^-2 with ZF–SIC, 1.58*10^-2 with ZF–SIC ordering and 4.8*10^-3 with ML detector. These shows that there is continuous performance improvement by using the non-linear (SIC and OSIC) detectors with lower complexity. This is true for the rest of antenna arrangements and their values are given in Table 6. The computational complexity of the ZF, ZF-OSIC and ML

detectors are respectively on the order of 1.05x10^3, 2x10^3 and 6.83x10^4 for QAM modulation and 2x2 V-BLAST system (Figure 3.10). The ML detector is around 35 times computational complex than ZF-OSIC for this antenna arrangement and modulation used. Also the average performance is improved when the number of receive antenna increases due to the additional receive diversity gain.

Table 6: Sample data (at constant SNR=8 & constant BER=10^-2) for ZF, ZF -SIC, ZF -SIC-Ordered & ML detectors

Antenna arrangement	BER at 8dB SNR				SNR in dB at BER of 10^-2			
	ZF	ZF -SIC	ZF -SIC-Ordered	ML	ZF	ZF-SIC	ZF-SIC-Ordered	ML
2X2	3.4*10^-2	2.2*10^-2	1.58*10^-2	4.8*10^-3	14	11.5	9.8	6.2
2X3	3.3*10^-3	1.8*10^-3	1.1*10^-3	5.15*10^-4	5.5	4.5	3.6	2.8
2X4	3.75*10^-4	2.15*10^-4	7.35*10 ^-5	2.5*10^-5	2.2	1.5	1	.8

D. Performance bound trends of RCPC codes

As shown in Figure 4.11, at 8dB, the BER is around 3.5x10^-7 with code rate of 8/30 while it is 1.45x10^-2 with code rate of 8/9. Thus, the lower code rates give the highest protection level. Also the RCPC codes using the same encoder/decoder can cover a SNR between 5 and 16.25 dB to achieve a BER of 10^-4 on Rayleigh channel. This means that the same link can serve users with a power margin variation of 11.25 dB by changing the code rate between 8/9 and 8/30 at the expense of throughput since the throughput is directly proportional to the code rate.

E. UEP performance analysis of RCPC encoded V-BLAST MIMO System

As shown in Figure 4.12, the code rates are varied from 8/9 to 8/30. It can be observed that as the rate of a code decreases, the error-protection level improves consistently. The system can provide a BER level of 10^-2 with SNR varying from approximately -2.5 dB to 5.4 dB by changing the code rate between 8/9 and 8/30 at the expense of throughput. The SNR range covered is narrower at lower levels of BER and by using the higher code rates for lower priority data bits, we can increase the bandwidth efficiency.

Chapter 5

Conclusion & Recommendation

5.1 Conclusion

Wireless communication systems with multiple transmit and receive antennas offer significant advantages in terms of increased data rates and reliability over those of single antenna systems. One of the main challenges facing V-BLAST systems is in receiver design to achieve higher data rates with acceptable computational complexity.

In this thesis, we investigate the performance of general V-BLAST MIMO architecture with ML, ZF, MMSE, SIC and the OSIC detectors & performance bound trends of RCPC codes with the mother code rate of ¼ and UEP analysis of RCPC encoded V-BLAST system. The performance (BER) and complexity of mathematical manipulation are compared. From the results (Figures 4.2, 4.3, 4.4, 4.5, 4.6, 4.7, 4.8, 4.9, 4.10) we have seen that that Maximum Likelihood (ML) is the best performing detector. But, its complexity grows exponentially with the number of transmit antennas and constellation used (Figures 3.10 & 3.11). Zero-Forcing is the least complex scheme but the performance is very low. By using the SIC & OSIC detectors, we approach the performance of the ML detector with less complexity cost. This high performance and lower complexity are achieved at the expense of a manageable latency. The average performance is also improved when the number of receive antenna increases due to the additional receive diversity gain. From Figure 3.11, the computational complexity of the ZF-OSIC, MMSE-OSIC and ML detectors are respectively on the order of 2x10^3, 2x10^3 and 6x10^4 for BPSK modulation and 2x2 V-BLAST system. The BER performace for MMSE-OSIC (Figure 4.7) and ZF-OSIC (Figure 4.10) is almost similar to the ML detector with more than 30 times computational complexity cost reduction (Figures 3.10 & 3.11). There is no need of using the ML detector to achieve lower bit error probability in this case. Therefore, A researcher or system designer should consider the performance versus complexity tradeoff

among the various V-BLAST detectors so as to determine the optimum choice in the face of his or her available constraints.

Furthermore, for the general V-BLAST systems with multiple antennas, error propagation is considered as the key problem to SIC. Thus, an ordered SIC detector is used to combat the influence of error propagation. The simulation outputs (Figures 4.5, 4.6, 4.7, 4.8, 4.9, 4.10) show the benefits of ordering strategy over Successive Interference Cancellation in terms of performance improvement.

The RCPC codes reduce the implementation complexity of a decoder and are very suitable for systems with unequal error protection and single channel codec structure. We have seen that the lower RCPC code rates provide good BER performance than the higher ones improving the error-protection level consistently (Figures 4.11 & 4.12) and the SNR range covered is narrower at decreasing levels of BER (Figure 4.12). We can increase the bandwidth efficiency by using the higher code rates for lower priority data bits.

5.2 Recommendation

We conclude with some brief remarks on future extensions of the work presented in this thesis.

- In this thesis we have considered the general V-BLAST systems that do not depend on knowledge of the the channel state information at the transmitter. Performance evaluation for the general V-BLAST systems with partial or full availability of the channel state information at the transmitter through some form of feedback mechanism and comparision of it with the unknown CSI at transmitter needs further research.
- By using the SIC & OSIC detectors, we approach the performance of the ML detector with less complexity cost. This high performance and lower complexity are achieved at the expense of a manageable latency and we consider that this latency has no impact on the BER performance & complexity. Dealing with the impact of latency on BER performance & complexity with these non-linear detectors (SIC & OSIC) is another recommended future reasearch area.
- Further researches are needed to clarify the significance of puncturing patterns to increase the free distance of RCPC codes and subsequently improve the BER performance of the RCPC codes.
- By changing the puncturing pattern of RCPC codes, we can gain a different value of power margin, BER improvement at the expense of throughput. Analyzing the impact of this puncturing pattern on the throughput and optimazation of the throughput− power margin & throughput-BER for RCPC encoded V-BLAST system is another recommended future reasearch area.

References

[1] David Tse and Pramod Viswanath, "*Fundamentals of Wireless Communication*," Cambridge Universtiy Press, 2005

[2] G.J. Foschini, "*Layered Space-Time Architecture For Wireless Communication in a Fading Environment When Using Multi- Element Antenna*," Bell Laboratories Technical Journal, pp. 41-59, Oct. 1996.

[3] J. Hagenauer, "*Rate-compatible Punctured Convolutional Codes (RCPC Codes) and Their Applications*," IEEE Trans. On Communications, vol. 36 no. 4, pp. 389-400, Apr. 1988, doi: 10.1109/26.2763

[4] Lydia Sari, Gunawan Wibisono, and Dadang Gunawan, "*Performance of RCPC-Encoded V BLAST MIMO In Nakagami-m Fading Channel*," JOURNAL OF TELECOMMUNICATION , VOLUME 2, ISSUE 2, MAY 2010.

[5] Andrea Goldsmith, "*wireless communication*," Stanford University, 2004.

[6] R. Guo, J. Liu, "*BER performance analysis of RCPC encoded MIMO-OFDM in Nakagami-m channels*," IEEE Conf. on Information Acquisition (ICIA 06), IEEE Press, Aug. 2006, pp 1416– 1420, doi: 10.1109/ICIA.2006.305963

[7] P.W. Wolniansky, G.J Foschini, G.D. Golden, and R.A. Valenzuela, "*V-BLAST: An Architecture For Realizing Very High Data Rates Over The Rich-Scattering Wireless Channel*," Proc. of URSI International Symposium on Signals, Systems and Electronics (ISSSE '98), pp. 295 – 300, Sep/Oct 1998, doi: 10.1109/ISSSE.1998.738086

[8] Branka Vucetic and Jinhong Yuan, "*Space-Time Coding*," John Wiley & sons Ltd, 2003.

[9] G.D. Golden, G.J. Foschini, R.A. Valenzuela and P.W. Wolniansky, "*Detection algorithm and initial laboratory results using V-BLAST space-time communication architecture*," IEE Electronic Letters, pp. 14–16, January 1999.

[10] Gerard J. Foschini and Michael J. Gans, "*On limits of wireless communications in a fading environment when using multiple antennas*," Wireless Personal Communications, 6(3):311–335, March 1998.

[11] J. Hagenauer, N. Seshadri, and C.-E. W. Sundberg, "*Variable-rate embedded sub band speech coding and matched convolutional channel coding for mobile radio channels*," in Proc. I988 IEEE Veh. Technol. Conf., VTC'88, Philadelphia, PA, June 1988, pp. 139-146.

[12] P. Kulakowski, "*The Multiple-Input Multiple-Output Systems in Slow and Fast Varying Radio Channels*," PhD Dissertation, AGH University of Science and Technology, Krakow, Poland, 2007.

[13] Yujin Noh, et.al., "*Design of Unequal Error Protection for MIMO-OFDM Systems*," IEEE 61st Vehicular Technology Conference, Vol. 2, May 30-June 1 2005, pp. 1058-1062.

[14] www.wireless-world reseach.org/fileadmin/files/about_the_forum/WG4/Briefings/WWRF WG4_smart_antennas_briefings.pdf

[15] NIRMALENDU BIKAS SINHA, R. BERA, M. MITRA, "*Capacity and V-BLAST techniques for MIMO wireless channel*," Journal of Theoretical and Applied Information Technology, 2010.

[16] John G.proakis, "*digital communications*", 4th edition, McGraw-Hill companies, 2001.

[17] A. J. Viterbi, "*Convolutional codes and their performance in communication systems*," IEEE Trans. Commun. Technol., vol. COM -19, pp. 751-772, Oct. 1971.

[18] E. G. Larsson and P. Stoica, "*Space-time block coding for wireless communication*," *Cambridge*, 2003.

[19] Dmitry Chizhik, Farrokh Rashid Farrokhi, Jonathan Ling, Angel Lozano, "*Antenna Separation and Capacity of BLAST in Correlated Channels*," IEEEAPS Conference on Antennas and Propagation for Wireless Communications, pp. 183–185, November 2000.

[20] J. G. Proakis and M. Salehi, "*Digital Communications*," Singapore: McGraw-Hill International, pp. 510 -516, 2008.

[21] S. Lin and D. J. Costello, Jr., "*Error Control Coding: fundamentals and Applications*,". Englewood Cliffs, NJ: Prentice-Hall, 1983.

[22] S. Verdu, "*Multiuser Detection*," Cambridge University Press, 1998.

[23] G. C. Clark, Jr. and J. B. Cain, "*Error-Correction Coding for Digital Communication,*" New York: Plenum, 1981.

[24] Farooq, M.S., et al., *"An Unequal Error Protection Scheme For Multiple Input Multiple Output Systems,"* in 36th Asilomar Conference on Signals, Systems and Computers, pp 575-579, 2002.

[25] T. S. Rappapot, *"Wireless Communications: Principles and Practice,"* Prentice Hall, 1996.

[26] M.Simon and M.S.Alouini, *"digital communication over fading channel,"* John & Sons Ltd, 2000.

[27] W.Yan and S.Sun, "*Iterative Interference Cancellation and Decoding for Convolutional Coded VBLAST Systems,*" Information, Communications and Signal Processing 2003, vol.3, pp.1511-1515, Dec 2003

[28] Stephen Baro, Gerhard Bauch, Aneta PAvlic, Andreas Semmler, *"Improving BLAST Performance using Space-Time Block Codes and Turbo Decoding,"* IEEE Global Telecommunications Conference, pp. 1067–1071, November 2000.

[29] Y. Yasuda, K. Kashdri, and Y. Hirata, *"High rate punctured convolutional codes for soft decision Viterbi decoding,"* IEEE Trans. Cornmun., vol. COM-32, pp. 315-319, Mar. 1984.

[30] Y. Jiang, X. Zheng, and J. Li, *"Asymptotic Performance Analysis Of V-BLAST,"* Proc. of IEEE Global Telecommunication Conference (Globecom '05), pp. 3882-3886, Dec. 2005, doi: 10.1109/GLOCOM.2005.1578497

[31] Lydia Sari, Gunawan Wibisono, and Dadang Gunawan, *"BER Performance Analysis of V-BLAST MIMO System with Joint Source and Channel Coding,"* IEEE Pacific-Asia Workshop on Computational Intelligence and Industrial Application, 2008.

[32] Y. Yasuda, Y. Hirata, *"Development of variable-rate Viterbi decoder and its performance characteristics,"* in Proc. 6th Znt. Con$ Digit. Satellite Commun., Phoenix, AZ, Sept. 1983, pp. XII-24-XII-31.

[33] George Tsoulos, *"MIMO SYSTEM TECHNOLOGY FOR WIRELESS COMMUNICATIONS,"* Published in 2006 by CRC Press Taylor & Francis Group.

[34] A. Hottinen, O. Tirkkonen, R. Wichman, *"Multi-Antenna Transceiver Techniques for 3G and Beyond,"* John Wiley and Son Ltd. 2003.

[35] A. Grant, S. Perreau, J. Choi and M. Navarro, *"Improved radio access for cdma2000,"* Technical Report A9.1, July 1999.

[36] Jin REN, *"Soft-Output Signal Detectors: Performance Comparisons in Multiple-Input Multiple-Output (MIMO) Systems,"* Journal of Computational Information Systems, December, 2010.

[37] R. Van Nee. A. Van Zelst, and G. Awater, *"Maximum Likelihood Decoding in a Space Division Multiplexing System,"* Proc. of VTC 2000, Vol. 1, pp. 6-10 Tokyo, Japan, May, 2000.

[38] J. B. Cain, G. C. Clark, and J. M. Geist, *"Punctured convolutional codes of rate (n - l)/n and simplified maximum likelihood decoding,"* IEEE Tram. Inform. Theory, vol. IT-25, pp. 97-100, Jan. 1979.

[39] I. E. Telatar, *"Capacity of Multi-antenna Gaussian Channels,"* AT&T Bell Laboratories, Technical Memorandum, June 1995.

[40] Albert van Zelst, *"MIMO OFDM for Wireless LANs,"* PhD Dissertation, Eindhoven university,14 april 2004.

[41] D. Gesbert, M. Shafi, D. Shiu, P. J. Smith and A. Naguib, *"From Theory to Practice: An Overview of MIMO Space–Time Coded Wireless Systems,"* IEEE Journal on Selected Areas in Communications, vol. 21, no. 3, pp. 281-302, April 2003.

[42] S. M. Alamouti, "*A simple transmit diversity techniques for wireless communications*," *IEEE J. Select Areas Commun.*, vol. 16, pp. 1451-1458, Oct. 1998.

[43] C. E. Shannon, *"A Mathematical Theory of Communication,"* The Bell System Technical Journal, vol. 27, pp. 379–423 and 623–656, July and October, 1948.

[44] Andrea Goldsmith, *" A Reduced-complexity MIMO Receiver via Channel Ordering,"* IEEE " GLOBECOM", Stanford University, 2009.

[45] W.H. Press, S. A. Teukolsky, W.T. Vetterling, and B.P. Flannery, *"Numerrical Recipes in C, The Art of Scientific Computing,"* Cambridge University Press, 1992.

[46] J. Hagenauer, *"Viterbi decoding of convolutional codes for fading and burst channels,"* in Proc. 1980 Int. Zurich Sem., Mar. 1980, pp. G2.1-G2.7

[47] JOACHIM HAGENAUER, *"The Performance of Rate-Compatible Punctured Convolutional Codes for Digital Mobile Radio,"* IEEE, 1990.

[48] Virtej, E., Kuusela, M. & Tuomaala, E. "*System Performance of Single-User MIMO in LTE Downlink*," in 19th IEEE Personal, Indoor and Mobile Radio Conference, pp. 1-5 , 2008.

[49] G.Strang, "*Linear Algebra and its Applications*," Third Edition, San Diego, Harcourt Brace Jovanovich, Publishers, 1988.